Bachelor's Thesis

BACHELOR'S DEGREE IN INDUSTRIAL TECHNOLOGY ENGINEERING

Analysis and design of passive assistive devices for patients with Duchenne Muscular Dystrophy

THESIS REPORT

Author: Paula Comas Triadó

Supervisors: Dr. Albert Peiret, Dr. Ofir Arad

Date: September 13, 2021

Escola Tècnica Superior
d'Enginyeria Industrial de Barcelona

Acknowledgments

The work presented in this thesis would not have been possible without all the people who supported me along the way, since I started studying this degree until today. I would like to thank everyone who has been by my side.

First of all, I would like to thank strongly my supervisor, **Dr. Albert Peiret**, who has guided me, helped me and solved all the problems and doubts every time I needed it. Moreover, I would like to thank **Dr. Josep Maria Font**, director of the BIOMEC Lab, who has also helped a lot with his feedback and knowledge. I really appreciate your confidence and trust in me to develop this project. And to the rest of the **BIOMEC Lab**: thank you very much, it has been an incredible experience, I deeply admire all of your work, and I am very grateful to have been part of this team.

I would also like to thank **Ofir Arad**, external supervisor and representative of Duchenne Parent Project Spain, for all the meetings, feedback, and guidance through the development of the thesis.

To **Dra. Julita Medina**, from Hospital Universitari Sant Joan de Déu, and **Oriol Alís** for contributing with their knowledge and helping me understand better the disease.

Also acknowledge that the data used in this thesis has been provided by the **Eurecat Foundation**, and they are the result of the **Exorapi project**, from the Exorapi consortium, a project funded by the Spanish Ministry of Economy, Industry and Competitiveness and by the European Union, within the framework of the Challenges-Collaboration call of the State Programme for Research, Development and Innovation Oriented to the Challenges of Society, as part of the State Plan for Scientific and Technical Research and Innovation 2013-2016.

Furthermore, I want to express my gratitude for having been granted the Santander-UPC Research Initiation Grant (INIREC).

Last but not least, thanks to my flatmates, who have closely followed the development of this thesis, and the rest of my friends and family for your infinite support during this journey, I would not have made it without you.

Abstract

Duchenne Muscular Dystrophy (DMD) is the most common form of muscular dystrophies diagnosed during childhood, and it affects approximately 1 out in 5000 male newborns in the world [1]. This disorder causes the progressive muscle weakness and loss of muscle mass, which leads to serious medical problems. Children with DMD usually have impairment in the upper limb, a characteristic gait pattern and several medical problems such as scoliosis, fractures and heart problems, among others. The first symptoms appear between 3 and 5 years old, and by the age of 12 the ability to walk is lost, and the children need to use a wheelchair. Orthopaedic devices and other assistive technologies, such as canes, braces and wheelchairs, are usually necessary to aid walking and posture.

This thesis aims to design a passive assistive device to improve the posture and gait of children with DMD through computational simulations and optimal control tools. Therefore, the thesis is focused on the late ambulatory stage, in which it becomes increasingly difficult for the children to walk, and it requires the use of orthopaedic devices like Ankle-Foot-Orthosis and Knee-Ankle-Foot-Orthosis. Although these devices are very helpful, they require time and commitment from the patient and the people who take care of them, additionally to the financial cost of the devices. For this reason, this thesis's purpose is to simulate and analyse the gait of children with DMD in order to identify the parameters to design a virtual prototype to assist them walking.

Two OpenSim models have been adapted to the size and properties of children from the age of nine, one healthy and one with DMD. The maximum isometric force of the muscles in the model with DMD has been modified to represent muscular dystrophy, and a general hyperactivation of the muscles has been obtained after performing *MocoTrack*. Subsequently, muscular dystrophy has been implemented in the healthy model and the activations have been limited with the purpose of forcing the reserve actuators to perform torque. Another *MocoTrack* has been carried out, and it has been found that the right iliopsoas muscle is at its maximum activation during the whole gait, and in the terminal stance and pre-swing periods the reserve actuator of the right hip performs a relatively high torque, which leads to the conclusion that the right iliopsoas needs assistance for hip flexion. The torque performed by the reserve actuator is then parameterized to three different springs using first order linear regressions. The springs have been tested and optimized, ultimately obtaining a spring that reduces the activation of most of the muscles and partially substitutes the performance of the reserve actuator.

Contents

Acknowledgments 1

Abstract 3

List of Figures 6

List of Tables 8

1 Introduction 11
- 1.1 Motivation . . . 11
- 1.2 Objectives and scope . . . 11
- 1.3 Project programming . . . 12

2 Theoretical background 15
- 2.1 Duchenne Muscular Dystrophy . . . 15
  - 2.1.1 General information . . . 15
  - 2.1.2 How DMD affects gait . . . 16
  - 2.1.3 Orthopaedic treatment . . . 23
- 2.2 OpenSim and OpenSim Moco . . . 24
  - 2.2.1 Musculoskeletal models . . . 24
  - 2.2.2 Musculoskeletal optimal control . . . 26
- 2.3 Lower limb passive assistive devices . . . 31
  - 2.3.1 Multidimensional springs system that can replace the muscle's torque during gait . . . 31
  - 2.3.2 Lightweight unpowered exoskeleton that reduces the energy cost of human walking . . . 32

3 Methodology 35
- 3.1 Lower limb musculoskeletal model . . . 35
  - 3.1.1 Description of the model . . . 35
  - 3.1.2 Modifications and scaling of the model . . . 36
- 3.2 Data processing . . . 38
- 3.3 Tracking of the movement . . . 39
  - 3.3.1 Problem definition . . . 39
  - 3.3.2 Solver definition . . . 41
  - 3.3.3 Solution . . . 41
- 3.4 DMD modelling . . . 41
  - 3.4.1 Decreasing of the maximal isometric force . . . 42
  - 3.4.2 Restriction of the muscle excitations . . . 43
  - 3.4.3 Tracking solution . . . 43

3.5 Design of the device . . . 44
3.5.1 Designed devices and implementation . . . 48
3.5.2 Tracking solution . . . 48

4 Results and discussion **49**
4.1 Tracking of the movement . . . 49
4.2 DMD modelling . . . 51
4.3 Design of the device . . . 51
4.4 Limitations of the thesis . . . 55

5 Economic cost of the project **57**

6 Conclusions **59**

References **61**

A Plots and results **65**
A.1 Tracking of the movement . . . 65
A.1.1 *DMD* model . . . 65
A.1.2 *CONTROL* model . . . 67
A.2 DMD modelling . . . 69
A.3 Design of the device . . . 71
A.3.1 SPRING 1 . . . 71
A.3.2 SPRING 2 . . . 73
A.3.3 SPRING 3 . . . 75

List of Figures

1 Gantt chart of the project. . . . 13
2 Iliopsoas, biceps femoris and gluteus maximus muscles [2]. . . . 18
3 Back and front view of the adductor muscles group [2]. . . . 18
4 Rectus femoris and the vastus muscle group [2]. . . . 18
5 Tibialis anterior, gastrocnemius and peroneus muscle [2]. . . . 19
6 Distance parameters on a person's footprints. Image extracted from [3]. . . . 19
7 Gait cycle terminology and phases of the gait. Image extracted from [4]. . . . 21
8 On the left, pelvis tilt [5]. On the right, plantarflexion and dorsiflexion movement of the ankle [6]. . . . 21
9 On the left, lumbar flexion and extension [7]. In the center, hip abduction and adduction movement [8]. On the right, first a knee with normal extension and secondly an hyper-extended knee [9] . . . 22
10 On the left, an Ankle-Foot orthosis. On the right, a Knee-Ankle-Foot orthosis. Source of the image: [10] . . . 24
11 Hill's muscle model [11] . . . 26
12 Overview of Moco. [12] . . . 27
13 Overview of *MocoStudy*. Moco can solve custom optimal control problems using a library of cost, boundary constraint, and path constraint modules.[13] . . . 28
14 How the *MocoSolutions* can be used as the initial guess for the following study [13]. 30
15 Solving prescribed motion, tracked motion, predicted motion problems and the Moco tool that each of these motions require. In order to predict a motion, which is a very common application in Moco, there is not a standardized tool. [13] . . . 31
16 Schematic model of the ExoNET for the right leg. . . . 32
17 Unpowered exoskeleton design from Collins et al. study. . . . 33
18 Front coronal, sagittal and back coronal planes of the model. . . . 36
19 Markers placement from the Exorapi Project [14]. . . . 37
20 Inverse Kinematics overview. . . . 38
21 *MocoTrack* tool. [13] . . . 39
22 Reserve actuators' performance in the *WEAKENED* tracking. The highest torque is applied by the reserve actuator in the right hip. . . . 44
23 Right muscles activity of the *WEAKENED* tracking. . . . 45
24 Plot of the reserve actuator's torque versus the joint angle for each joint and their respective lineal regressions. The blue line is the right hip reserve actuator's torque, and the red line is the obtained lineal regression. . . . 46
25 Plot of the right hip reserve actuator's torque versus the joint angle for each gait cycle phase. The blue line is the right hip reserve actuator's torque, the red line is the obtained lineal regression for each phase, and the black line is the lineal regression for the whole gait. . . . 47

26 Lineal regression excluding the data from the midstance and terminal stance phases. The blue line is the right hip reserve actuator's torque, and the red line is the obtained lineal regression. 48
27 $\%RMS$ values of the trackings of *DMD* and *CONTROL* models. 50
28 Mean muscle activations of the trackings of *DMD* and *CONTROL*. 50
29 Mean reserve actuator torque in the *DMD* and *CONTROL* trackings. 50
30 $\%RMS$ values of the trackings of *CONTROL* and *WEAKENED* models. 51
31 Mean values of the muscles activations in the *CONTROL* and *WEAKENED* trackings. 52
32 Torques applied by the reserve actuators in the *CONTROL* and *WEAKENED* trackings. 52
33 Percentage of the RMS with respect to the reference range of motion in each tracking. 53
34 Muscles activations in each tracking. 53
35 Muscles activations in *CONTROL* and *SPRING 2* tracking. 54
36 Reserve actuators' performance in each tracking. 54

List of Tables

1 Characteristics of the data that was used for the models. . . . 38
2 Forces normalized by weight for each patient in the study. HF stands for Hip Flexion, HE for Hip Extension, KF for Knee Flexion, KE for Knee Extension, AF for Ankle Flexion (also known as dorsiflexion) and AE for Ankle Extension (also known as plantarflexion). . . . 42
3 Normalized and non-normalized force scales. The normalized scale is calculated with the formula 9 and the non-normalized scale with the formula 10. . . . 43
4 Torque values of the reserve actuators in the *WEAKENED* tracking. The actuator with the highest torque is the one in the right hip. . . . 44
5 Parameters obtained from the first degree lineal regression for each reserve actuator. The row of the right hip reserve actuators is highlighted in yellow. . . . 46
6 Parameters obtained from the first degree lineal regression of the right hip reserve actuator's torque, from the 50% to the 100% of the gait cycle. . . . 47
7 Parameters of the three designed springs . . . 48
8 Parameters of the chosen spring. . . . 54
9 Economic cost of the project . . . 57
10 Root Mean Square of the coordinates of the *DMD* tracking, the range of motion of the reference in each coordinate, and the percentage of the RMS respect the range of motion. . . . 65
11 Torque values of the reserve actuators in the *DMD* tracking. . . . 65
12 Right and left muscle activations in the *DMD* tracking. . . . 66
13 Root Mean Square of the coordinates of the *CONTROL* tracking, the range of motion of the reference in each coordinate, and the percentage of the RMS with respect to the range of motion. . . . 67
14 Torque values of the reserve actuators in the *CONTROL* tracking. . . . 67
15 Right and left muscle activations in the *CONTROL* tracking. . . . 68
16 Root Mean Square of the coordinates of the *WEAKENED* tracking, the range of motion of the reference in each coordinate, and the percentage of the RMS with respect to the range of motion. . . . 69
17 Right and left muscle activations in the *WEAKENED* tracking. . . . 70
18 Root Mean Square of the coordinates of the *SPRING 1* tracking, the range of motion of the reference in each coordinate, and the percentage of the RMS with respect to the range of motion. . . . 71
19 Torque values of the reserve actuators in the *SPRING 1* tracking. . . . 71
20 Right and left muscle activations in the *SPRING 1* tracking. . . . 72
21 Root Mean Square of the coordinates of the *SPRING 2* tracking, the range of motion of the reference in each coordinate, and the percentage of the RMS with respect to the range of motion. . . . 73

22 Torque values of the reserve actuators in the *SPRING 2* tracking. 73
23 Right and left muscle activations in the *SPRING 2* tracking. 74
24 Root Mean Square of the coordinates of the *SPRING 3* tracking, the range of motion of the reference in each coordinate, and the percentage of the RMS with respect to the range of motion. 75
25 Torque values of the reserve actuators in the *SPRING 3* tracking. 75
26 Right and left muscle activations in the *SPRING 3* tracking. 76

1 Introduction

1.1 Motivation

This thesis has been developed in the BIOMEC Lab in collaboration with Duchenne Parent Project España (DPPE), a non-profit association created and run by parents of boys with Duchenne Muscular Dystrophy (DMD) and Becker Muscular Dystrophy (BMD). They work to find a cure or treatment for DMD and BMD, and to improve the quality of life of those affected and their families by promoting and funding clinical research, psychosocial care services, awareness campaigns and educational programmes.

In this context, DPPE was interested in the analysis and design of a simple assistive device, alternative to the commonly used to treat DMD, that assist walking and extend the ambulatory. The device should be designed for children around 10 years old, who are usually in the late-ambulatory stage and struggle to walk.

Thanks to the knowledge and technological tools used in the BIOMEC Lab, it was possible to create biomechanical models of children with DMD, reproduce the movement, analyse it and optimize the device's parameters. The data used to develop the thesis was given from the research project Exorapi, carried out by Hospital Infantil Sant Joan de Déu, CSIC-UPM, Eurecat and the advice of DPPE, among others.

1.2 Objectives and scope

The main goal of this thesis is to design a passive assistive device to assist walking in children with DMD. In order to achieve it, it has been subdivided to specific objectives.

- In order to develop hypotheses on how to implement muscular dystrophy in the musculoskeletal model, it is necessary to **understand how the disease affects muscles and gait.**
- Using the experimental data that was provided, different analyses need to be carried out in order to **adapt the models**, prepare and **test the simulations**. Subsequently, the developed simulations need to be **validated with the experimental** data and other studies.
- In order to achieve an accurate representation of **muscular dystrophy in the model**, different hypotheses on how to implement it need to be developed and tested.
- Once the model is properly modified to simulate the muscular dystrophy, the tracking needs to be analysed in order to **design the device**. Subsequently, the device is implemented in the model and an analysis of its impact is carried out

This thesis is a first approach to modelling muscular dystrophy in musculoskeletal models,

obtain proper simulations using optimal control and design a simple device for one joint that would help the gait of a child with DMD of a specific age.

1.3 Project programming

In order to develop this thesis, a Gantt chart has been designed taking into consideration the objectives and scope of the thesis, and the resources available at the time. As shown in Figure 1, the project is structured in six tasks, which will be explained in detail in the following text.

1. **Theoretical background**. During this period, research about DMD and assistive devices for children with reduced mobility has been carried out. Regarding DMD, the research is focused mainly on how the illness affects the gait in terms of biomechanical parameters such as muscular weakness, spatiotemporal parameters, kinematic and kinetic parameters and muscle activity. As for the assistive devices for children with reduced mobility, the research is focused on lower limb devices since the main interest of the thesis is to assist walking in children with DMD.

2. **Getting used to the environment**. Since the software and technological resources used in BIOMEC Lab were new to the student, it was needed a learning period through classes, tutorials, and autonomous work. The first software used is OpenSim [15], a software platform for modelling human biomechanics and simulate is their movement and interaction with the environment. Then, OpenSim Moco was used with Matlab to solve optimal control problems for musculoskeletal systems defined in OpenSim.

3. **Scaling and modifications of the models**. Certain modifications need to be made in the models so that they fit with the experimental data and correctly represent children.

4. **Tracking of the movements**. The approach of this thesis is to use *MocoTrack*, which allows observing how changes in different parameters of the model or the optimization affect the tracking of a given movement. The first tracking that is carried out is the tracking of the experimental data using the adapted models, which needs some adjusting to find the appropriate parameters.

5. **DMD modelling** In order to implement muscular dystrophy in a model, hypotheses need to be developed and tested.

6. **Design of the device**. Using the results of the simulations with the model with dystrophy, a device is designed and tested.

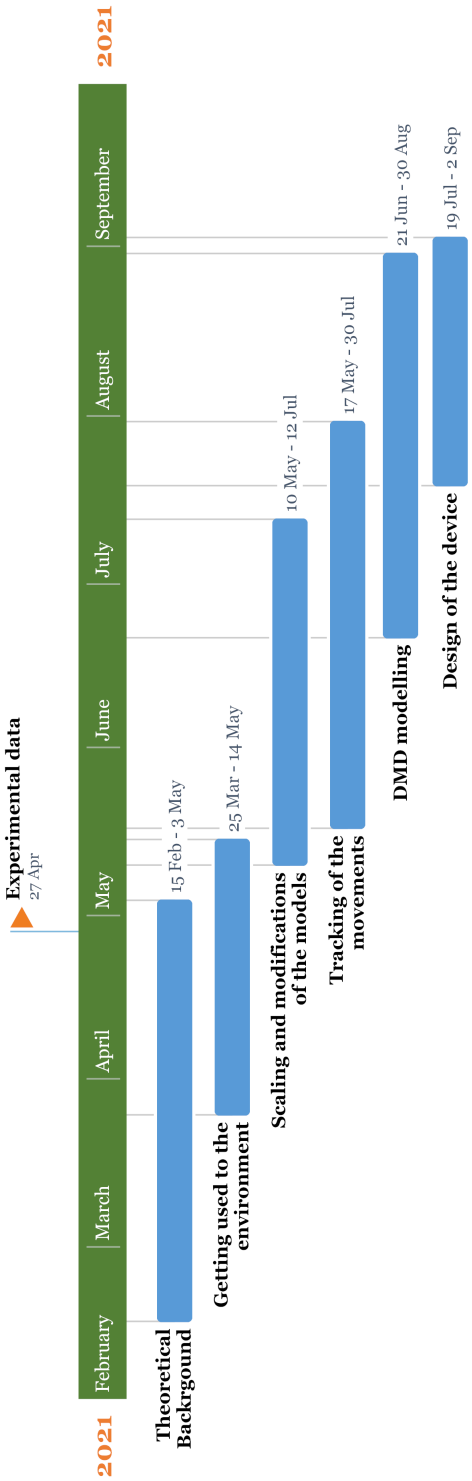

Figure 1: Gantt chart of the project.

2 Theoretical background

In this section, an overview on DMD and how it affects gait and muscles, the theoretical basis of OpenSim and OpenSim Moco, and two examples of passive assistive devices is exposed.

2.1 Duchenne Muscular Dystrophy

2.1.1 General information

Muscular dystrophies are hereditary diseases that cause progressive muscle weakness (myopathy) and loss of muscle mass (atrophy). They are typically caused by defects in proteins, which lead to the death of muscle cells and tissue. The most common form of muscular dystrophy (MD) is Duchenne Muscular Dystrophy (DMD), but there are other forms such as Becker, limb-girdle and congenital, among others.

DMD is the most common MD diagnosed during childhood, and it is caused by mutations in the dystrophin protein, which is located in the X chromosome. This gene is responsible for producing a protein called dystrophin, which normally protects muscle fibers: without dystrophin, muscles are broken down by enzymes, which cause degeneration and ultimately weakness of muscles. Because DMD is inherited in an X-linked recessive pattern, it manifests mainly in males. The mutation of the gene is usually transmitted from mother to child, but it may also occur by spontaneous mutations. [16]

The first symptoms of DMD usually appear in children between two and three years, and they need to use a wheelchair by the age of twelve or thirteen. The stages of the disease are [17] [18]:

- **Stage 1: Presymptomatic.** Between two and three years of age, symptoms of delayed walking or delayed speech appear, but are they typically subtle enough to be unnoticed or unrecognized at this stage.

- **Stage 2: Early Ambulatory.** Between three and five years of age, first signs of DMD appear, such as Gowers'manoeuvre[1], waddling gait [2] and walking on their toes. They are able to climb stairs, but they usually bring the second foot up to join the first rather than going foot over foot.

- **Stage 3: Late Ambulatory.** During the late childhood or adolescence, walking becomes increasingly difficult for the children and there are more problems with climbing stairs and getting up from the floor. Rehabilitation input is necessary in order to maintain the

[1] **Gower's sign** (manoeuvre) is a manoeuvre used by patients with muscular weakness to arise from a supine or seated position on the floor. In other words, they need to support themselves with their hands on the tights to get up from the floor of from squatting [19].

[2] **Waddling gait** is a gait disorder characterised by wide-based steps, swaying or rolling from side to side, and toe-walking, and it is due to myopathy and other neuromuscular disorders. [20]

range of motion and independence of the children. Sometimes orthopaedic specialists are necessary and appropriate wheelchairs with supportive seating are recommended to promote continued independence and comfort.

- **Stage 4: Early Non-Ambultory.** During the teenage years, people with DMD need to use a wheelchair and are usually able to wheel it themselves. Their posture is still good, although spinal curvature (scoliosis) is likely to appear and progress rapidly.

- **Stage 5: Late Non-Ambulatory.** As the teen transitions to adulthood, the disease worsens. Maintenance of good posture and upper limb function becomes increasingly difficult and complications are more likely.

Fractures involving the arms and legs are frequent, usually caused by falling; DMD can also cause heart problems such as enlargement of the heart tissue (dilated cardiomyopathy) and irregular heartbeat. Scoliosis, combined with muscle weakness, can lead to lung function problems. Steroid treatment is widely used in children with DMD in order to slow down the decline in muscle strength and motor function in DMD.

2.1.2 How DMD affects gait

Even though many studies have been carried out over the last years, there are some discrepancies on how DMD gait deviates from the typical gait pattern. The differences between the studies might be due to the progressive nature of the disease, which makes it difficult to give an accurate description of the gait alterations for a group of patients of different ages. The different methods and materials used in each study could also explain these discrepancies. [21]

However, the study of Gaudriaan et al. [21] [22] includes a systematic review of the gait deviations in DMD that were found in different studies. This systematic review will be used as a guideline to explain the most common gait deviations in children with DMD. Additionally, the information has been verified and complemented with the results of the studies carried out by Eurecat within the framework of the Exorapi Project [23].

Muscular weakness, spatiotemporal parameters, changes in kinematics and kinetic parameters, muscle activity and muscle activation will be described in the following text.

Muscular weakness

Although a direct association between muscle weakness and the gait deviations in children with DMD has not yet been reported [22], it does not mean that muscle weakness has no influence on the gait of these children. The most common hypothesis is that muscle weakness acts as a biomechanical constraint in the motion control of gait [24], meaning that, when muscles start to weaken, the child uses compensatory movements in order to maintain their posture during

gait; these compensatory movements modify their gait pattern. It is important, then, to have information about the weakness of the muscles in order to understand the alterations of the gait in children with DMD.

An overall muscular weakness is found in all the muscle groups of the lower limbs in patients with DMD. The muscle groups depend on the movement they act on:

- The **hip flexion** is the motion that brings the knee toward the chest, and the major hip flexor muscle is the iliopsoas (Figure 2), which includes the psoas major, psoas minor and iliacus.
- The **hip extension** is the motion that brings the thight from a flexed position towards the midline of the body. The major hip extensors muscles are the gluteus maximus and the biceps femoris (Figure 2).
- The **hip adduction** is the motion that brings the leg from a lateral position to its more axial alignment. The main hip adductors are the adductor magnus, the adductor brevis and the adductor longus (Figure 3).
- The **hip abduction** is the opposite movement of the hip adduction, it brings the leg from the axial alignment to a lateral position. The main hip abductor muscles are the gluteus medius, the gluteus minimus and the tensor fasci lata.
- The **knee flexion** motion is the bending of the knee from the straight position, and the muscles that perform knee flexion are referred to as the hamstring muscles, and they are located in the back of the thigh. The hamstring muscles include the biceps femoris (Figure 2), the semitendinosus and the semimembranosus.
- The **knee extension** motion increases the angle of the knee, bringing the lower leg from bending into a straight position. The knee extensor muscles are referred to as the quadriceps femoris, and they include the vastus medius, vastus lateralis, vastus intermedius and rectus femoris (Figure 4).
- The **dorsiflexion** is the ankle flexion in the direction of the dorsum, which is the anterior surface of the foot, and it is accomplished mainly by the tibialis anterior, the extensor digitorum longus and the peroneus muscle, also called fibularis muscle (Figure 5).
- The **plantarflexion** is the flexion of the ankle in the direction of the sole of the foot, and it is mostly accomplished by the calf musculature: the gastrocnemius (Figure 5) and the soleus.

The statistically significant weakness of the muscles has been found in tibialis anterior, peroneus, the biceps femoris and the whole adductors muscle group [25]. It has also been found a

significant weakness in the iliopsoas muscle, the rectus femoris, the gluteus maximus, and the gastrocnemius muscles. [26] (Figures 2, 3, 4 and 5)

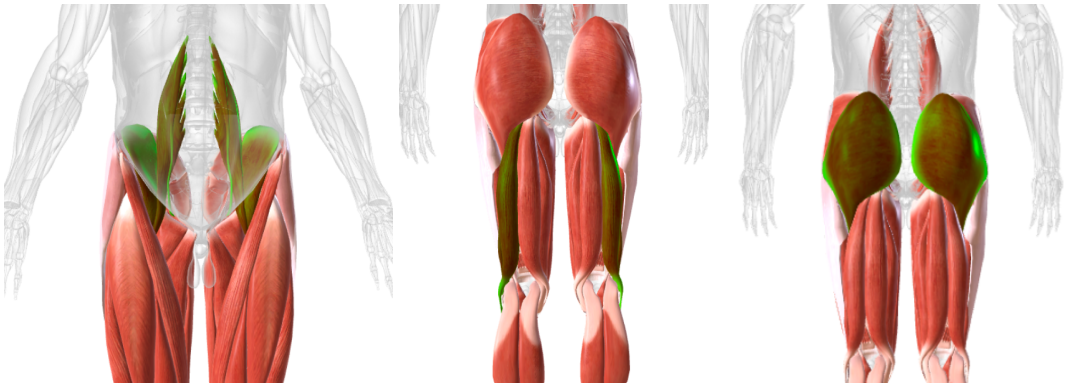

Figure 2: Iliopsoas, biceps femoris and gluteus maximus muscles [2].

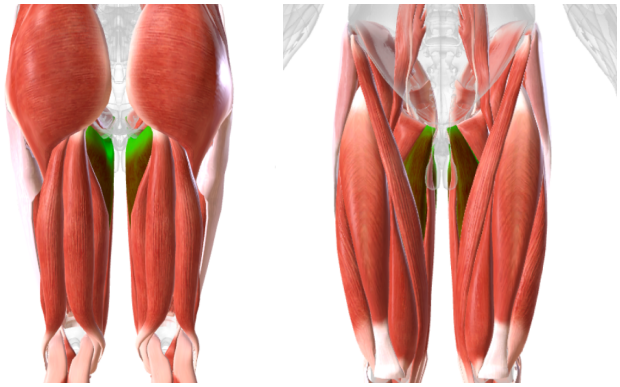

Figure 3: Back and front view of the adductor muscles group [2].

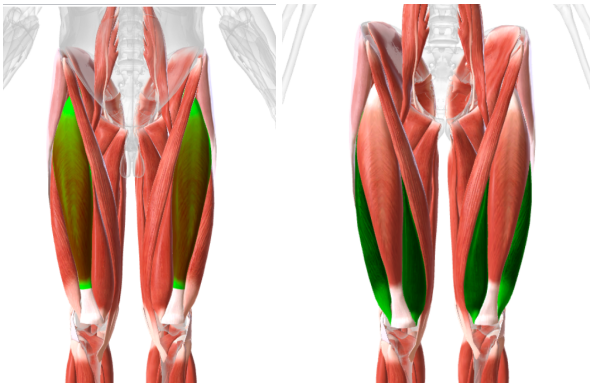

Figure 4: Rectus femoris and the vastus muscle group [2].

Figure 5: Tibialis anterior, gastrocnemius and peroneus muscle [2].

Regarding the progressive nature of the disease, the muscles that weaken in the first phase seem to be the gluteus maximus, the tibialis anterior, the quadriceps femoris and the gastrocnemius [27] [28].

Spatiotemporal parameters

It has been found that the **stride length**, which is the distance covered by one step with each foot, decreased in children with DMD. The **step length** is also lower in DMD children, and the study of D'Angelo et al. [26] found significant differences on the **step width** as well, showing an increased value on DMD children (Figure 6).

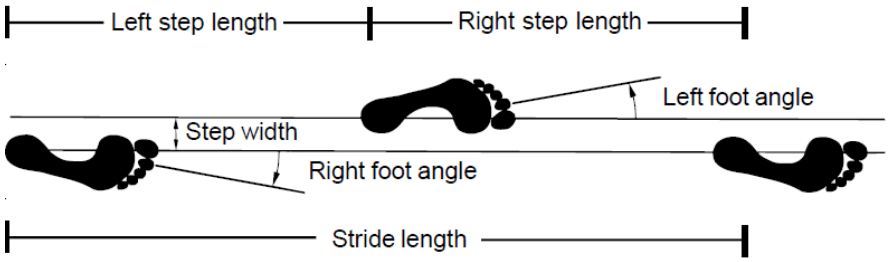

Figure 6: Distance parameters on a person's footprints. Image extracted from [3].

Contrary to what some studies have found [25], the cadence and walking speed of children with DMD are not significantly different from healthy children [26] [29]. The differences found in the aforementioned studies were in non-normalized spatiotemporal parameters, and this could have influenced the outcomes. It is important to take into consideration the subject's anthropometry when analysing the gait. For instance, children with DMD have a short stature and increased body-weight compared to age-matched healthy children due to the long-term use of corticosteroids. Therefore, their walking speed is lower than healthy children.

Changes in kinematic and kinetic parameters

To understand the changes in kinematics and kinetic parameters, it is necessary to understand the gait cycle and its phases. The gait cycle starts when one foot makes contact with the ground, and it ends when the same foot makes contact with the ground again. Usually, the gait cycle is divided into two phases: **stance phase**, when the foot is in contact with the ground, and **swing phase**, when the same foot is in the air. The separation between these two phases is discerned by the **toe-off**, which, in a healthy gait, usually happens at 60% of the gait cycle (GC).

During the stance phase, we can observe four periods:

- **Loading response**: between the initial contact and the opposite toe off (0 to 10% of GC);
- **Mid-stance**: between the opposite toe off and the heel rise (10-30% of GC);
- **Terminal stance**: between the heel rise and the opposite initial contact (30 to 50% of GC);
- **Pre swing**: between the opposite initial contact and the toe-off (50 to 60% of GC).

During swing phase, we observe three periods:

- **Initial swing**: between the toe-off and the feet adjacent (60 to 73% of GC);
- **Mid-swing**: between the feet adjacent and the tibia vertical (73 to 87% of GC);
- **Terminal swing**: between the tibia vertical and the next initial contact (87 to 100% of GC).

As shown in Figure 7, during the gait cycle different events can also be identified, such as initial contact (0% of GC), opposite toe off (10% of GC), heel rise (30% of GC), opposite initial contact (50% of GC), toe off (60% of GC, the changing point between phases), feet adjacent (73% of GC), and tibia vertical (87% of GC).

When looking at the changes in kinematic and kinetic parameters during the gait of children with DMD, it is shown an **increased total range of motion at the knee**; a **decreased dorsiflexion during swing**; a decreased maximal power generation at the hip and at the end of stance, and at the ankle before push-off; and a decreased maximal net knee extension torque and dorsiflexion torque during stance. [21].

The hypothesis developed by Eurecat in the framework of the Exorapi Project offers an explanation of how muscular dystrophy causes these changes in body posture and gait kinematics. The first affected muscles are the hip extensors, mainly the gluteus maximus. Consequently, the hip flexor muscles contract and produce a **pelvis anterior tilt** (Figure 8), which shortens the tensor fasci lata, and **lumbar flexion** (Figure 9), which causes an aggressive lumbar lordosis and a hyperextension of the vertebral column. The following affected muscles are the knee

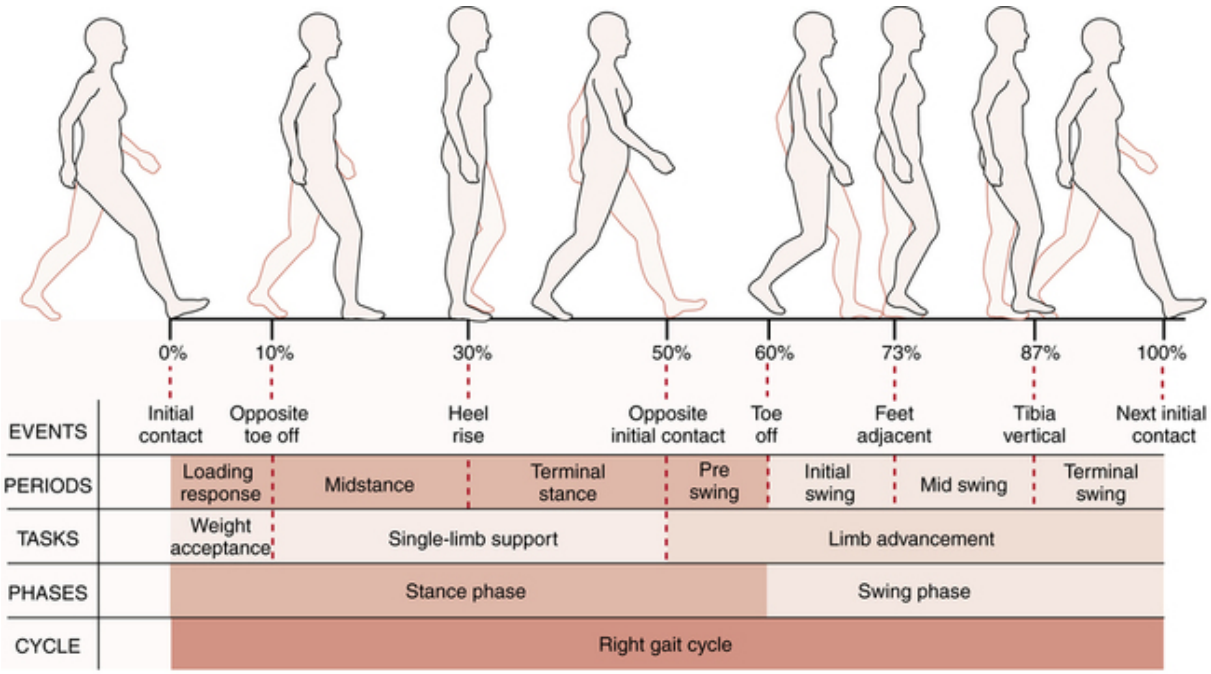

Figure 7: Gait cycle terminology and phases of the gait. Image extracted from [4].

extensors, which causes the child with DMD to adopt a **plantar flexion position** (Figure 8) in order to keep the weight in line with the knees and maintain the passive knee stability. These type of contractions progress during the ambulant phase, thus decreasing the base support. To the extent that the balance is lost, the child with DMD compensates with the **abduction of the hip** (Figure 9), resulting in a greater shortening of the tensor fasci lata.

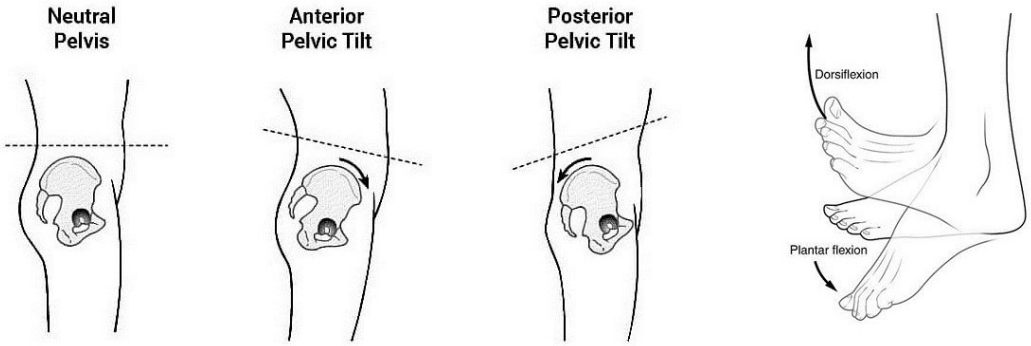

Figure 8: On the left, pelvis tilt [5]. On the right, plantarflexion and dorsiflexion movement of the ankle [6].

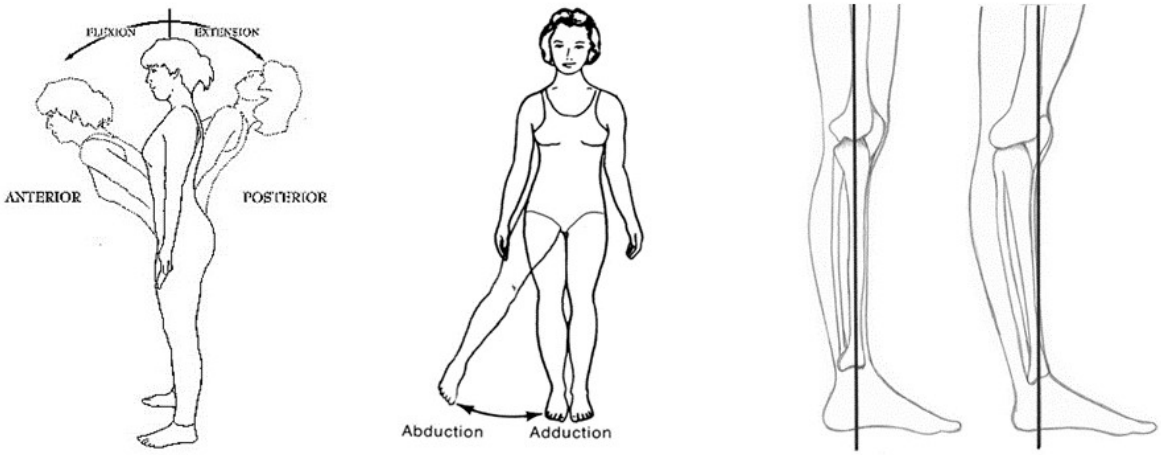

Figure 9: On the left, lumbar flexion and extension [7]. In the center, hip abduction and adduction movement [8]. On the right, first a knee with normal extension and secondly an hyperextended knee [9]

Regarding the gait cycle and considering the **progressive nature of the disease**, the first kinematic differences are small: an excessive plantarflexion during the swing with an increased hip flexion in order to step the foot forward. The cadence might be reduced, and the initial contact (0% GC) is made with the whole flat surface of the foot in order to minimize the hip and knee flexion moments during the stance phase. With the progression of the disease, the cadence keeps decreasing, the weakness of the gluteus medium increases and the shortening of the tensor fasci lata causes an excessive lumbar tilt and the adoption of a wider base support. Furthermore, the children with DMD learn to position themselves in a way that the weight line is above the knee, thus abandoning the knee flexion at the beginning of the stance phase and accommodating on the weakened knee extensors, causing **knee hyperextension** (Figure 9) in most cases. At the same time, in order to obtain stability, an increase of the plantarfleixon is made as the muscles' weakness progresses [30] [14].

Muscle activity

The underlying patterns of muscle activity in children with DMD have been little studied, and therefore there is a lack of understanding of the specific role of each lower limb muscle in the abnormal gait pattern. For this reason, it is of particular interest the study carried out by Ropars et al. [31], in which they compared the muscle activation and coactivation in the lower limbs during the gait cycle between children with DMD with healthy children of the same age and gender, and also explored the relationship between the muscle activation, lower limb kinematics and functional status.

The results of the aforementioned study confirmed quantitatively that the principal muscles of both lower limbs are **hyper-active** during gait in children with DMD. The increased activity of

the tibialis anterior (TA), hamstrings (HS) and rectus femoris (RF) is likely compensatory since the motor command is intact in these children. Furthermore, it was found that the amount of compensation (hyper-activity) was positively correlated to the severity of the functional status and the gait pattern, meaning that **the muscle hyper-activity during gait increased with the progression of the disease**. Particularly, the increase in percentage activation relative to the maximum recorded activation during gait could be the result of an increase in muscle fiber recruitment to compensate for weakness in the recorded muscle. This means that **muscle weakness would be compensated by an increase in muscle activity** in children with DMD. This suggests that, to produce the same levels of force, children with DMD need greater muscle activity.

Regarding the coactivation of the muscles, it was found significantly more coactivation between RF and HS during the whole of the gait cycle in the children with DMD, but there was no significant difference between groups for the VL/HS pair. There was also significantly more coactivation between TA and GAS in the children with DMD, particularly during stance. It is believed that the coactivation in children with DMD could be a **strategy to increase stability around the knee and ankle.** Coactivation of the knee muscles likely helps the child to maintain the center of gravity behind the hips and in front of the knees.

Despite the fact that TA was found to be moderately weak, it is the muscle with the most abnormal activity. Moreover, there was a decrease in muscle activity of TA in the children with DMD at the end of the gait cycle compared to healthy children. The hypothesis is that the hypoactivity could be anticipatory of foot-strike by the forefoot, and it would also explain the fact that there was a relative hyper-activity of GAS during the initial part of the stance. This suggests that forefoot contact (also known as "toe-gait"), which is characteristic of gait in children with DMD, is a compensatory mechanism to increase stability. The results found in this study [31] could invalidate current treatments applied to reduce equinus foot, such as surgery or splints, in children with DMD.

Taking all this results into account, and focusing on the goal of this thesis, Ropars et al. support the idea of avoiding muscular fatigue in children with DMD. They claim that **simple therapeutic solutions**, such as targeted physiotherapy or ankle-foot orthoses, could improve stability and reduce abnormal muscle activity in children with DMD. [31]

2.1.3 Orthopaedic treatment

The current orthopaedic treatment for people with DMD varies according to the stage of the disease. Since the early ambulatory stage, wheelchairs are needed for long distances in order to keep the strength. Furthermore, AFOs (Ankle-Foot Orthosis) are recommended during night in order to help control the ankle contractures since the early stages of the disease. At the point when walking becomes very hard or almost impossible (in the late-ambulant stage), KAFOs (Knee-Ankle-Foot Orthosis) are recommended in order to help control the joint stiffness, pro-

long ambulation and delay the onset of scoliosis. After this point, when walking is not possible anymore, powered or unpowered wheelchairs are needed for everyday life.[10].

Figure 10: On the left, an Ankle-Foot orthosis. On the right, a Knee-Ankle-Foot orthosis. Source of the image: [10]

2.2 OpenSim and OpenSim Moco

2.2.1 Musculoskeletal models

OpenSim is a software platform for modelling humans, animals, robots and the environment, and simulating their interaction and movement. In OpenSim, the human body is modelled as a multibody system with rigid bodies linked by ideal joints, with muscles and generalized coordinates. The rigid bodies represent the motion of the bones or group of bones, and the joints define the relative motion between segments by constraining certain degrees of freedom. The description of the configuration of a multibody system is done by defining a set of generalized coordinates associated with the angles and relative positions between the solids that compose it. In OpenSim, the **generalized coordinates** are the rotations allowed by the constraints between the solids [32].

In the following text, the most important components of musculoskeletal models in OpenSim will be briefly explained. More information can be found in the OpenSim Documentation [15].

Rigid bodies and joints

An OpenSim **body** represents the geometry and inertial properties of the body segments. Each body has its reference frame with associated inertia, which is specified by its mass, center of mass location in the reference frame, and its inertia tensor about the center of mass. The geometry and set of parameters of each rigid body in the model are specific and can be modified.

An OpenSim **joint** connects two bodies or frames and specifies their relative motion as described in internal coordinates. The relative motion is defined by specific joints, which describe the

permissible kinematics of a child[3] joint frame (on a child body) with respect to a parent joint frame (on a parent body). Each joint has six relative permissible motions: three translations around the joint's relative $x-$, $y-$ and $z-axis$, and three rotations about the joint's relative $x-$, $y-$ and $z-axis$ (these axes correspond to the parent body) [33]. The rotation about the relative $x-axis$ is usually called abduction, about the relative $y-axis$ rotation, and about the relative $z-axis$ flexion. There are several types of joints, and the three that have been used in this thesis are described in the following text.

- The **pin joint** provides one degree of freedom about the common $z-axis$ of the joint frames in the parent and child bodies.
- The **custom joint** is a generic joint representation. Its behaviour is specified by its spatial transform, which can be either one of the 3 rotations or one of the 3 translations that define the spatial position of the child frame with respect to the parent frame as a function of coordinates. An example of this joint is in the toes, since the axis about which they rotate with respect to the calcaneus is not a base axis.
- The **weld joint** allows no relative motion of bodies, which means that the child body is fixed to the parent body. This kind of joint is often used to create composite bodies from smaller, simpler bodies.

Most of the models have a tree topological structure, which means that there is a base segment(usually the pelvis) the motion of which is parametrized by three Cartesian coordinates and three angular coordinates (Euler angles). The other segments are connected to the base segment and their motions are parametrized by joint coordinates relative to the parent segment in the tree [11].

Muscles and nervous system

The geometry of the **muscles** in OpenSim is described by a line, and the two endpoints of the line, which represent the tendons attachments to the bones and are fixed to different rigid bodies. Some muscles have additional path points within the line, which allows representing better the actual muscle geometry.

Muscle fibers contract to generate force. The Hill-type muscle model [34], represents the muscle with a contractile element (CE), which represents the muscle fibers, and two elastic elements, one in parallel and another in series, which represent the connective tissue and the tendons, respectively (see Figure 11 for the representation of Hill's muscle model).

[3] A designation of child/parent is used to identify the directionality of the joint and in which frame the joint coordinates are expressed.

The muscle's activation $a \in [0, 1]$ is the fraction of fibers contracted in a muscle. The force generated by a contractile element can be written in terms of the muscle activation, the muscle fiber length l_M and the muscle fiber velocity $v_M = \frac{\mathrm{d}l_\mathrm{M}}{\mathrm{d}t}$, as shown in Equation 1. F^0_M is the maximum isometric force of the muscle, f_L and f_V are characteristic functions of the muscle that depend on the muscle parameters, and f_PE is the force of the parallel elastic element.

$$F_\mathrm{M} = F^0_\mathrm{M} \left(a \cdot f_\mathrm{L} \left(l_\mathrm{M} \right) f_\mathrm{V} \left(v_\mathrm{M} \right) + f_\mathrm{PE} \left(l_\mathrm{M} \right) \right) \tag{1}$$

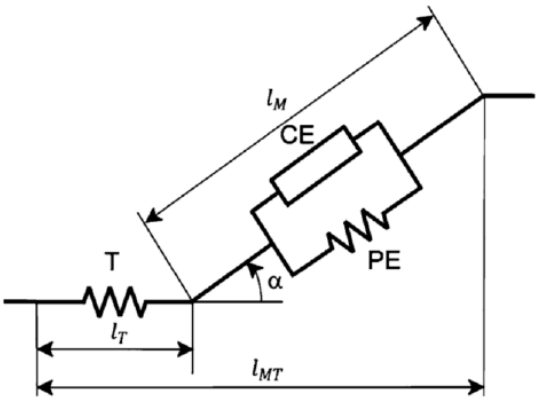

Figure 11: Hill's muscle model [11]

The **central nervous system** controls the muscles by sending an electric signal to contract the muscle fibers. To represent the neural commands, the neural excitation $e \in [0, 1]$ is used in each muscle. The neural excitation governs the muscle activations dynamics, which is described by a first-order system as shown in Equation 2. a is the muscle activation, and $\tau(e, a)$ is the activation time rate of the muscle fibers, which takes different values in case of fiber activation and deactivation.

$$\frac{\mathrm{d}a}{\mathrm{d}t} = \frac{e - a}{\tau(e, a)} \tag{2}$$

As explained in the previous chapters, the muscle's maximum isometric force of people with DMD is reduced and the activations are higher. Nevertheless, the neural excitations are unaltered, since DMD is not a neurological disease.

2.2.2 Musculoskeletal optimal control

Musculoskeletal simulations of movements can provide very useful information that can help humans regain mobility after injuries, design exoskeletons and other devices for rehabilitation. These simulations have already shed light on movement disorders by, for example, discovering ways to walk that reduce knee loading, revealing that children with cerebral palsy exhibit sim-

plified motor control when walking, and reproducing eye disorders that cause double vision. **OpenSim Moco** is a software toolkit for optimizing the motion and control of musculoskeletal models built in OpenSim that is able to handle a wide range of problems, including motion tracking, motion prediction, parameter optimization, model fitting, electromyography-driven simulation, and device design. It is worth noting that Moco is the first musculoskeletal direct collocation tool to handle kinematic constraints, which are common in musculoskeletal models [13].

As it is shown in the Figure 12, the inputs that can be introduced in Moco are the OpenSim model, the data collected from markers, force plaques or muscle activity, and the goals. The goals, such as tracking of markers, minimization of the effort or the joint loading, can be enforced either as cost terms or boundary constraints, and they define and limit the cost function, which is what the software optimizes in order to get the output. The output of the solver are the motion, the controls, and the parameters outputs.

Figure 12: Overview of Moco. [12]

Moco solves optimal control problems that users define using a library of cost and constraint modules, which are implemented through configurable software classes. These classes are available via C++, Matlab, Python and XML text files, and in this thesis the interface used has been **Matlab**. To describe the problem, the class used is *MocoProblem*, and to decouple the problem from the numerical methods used to solve it, the *MocoSolver* class is used. The *MocoProblem* and *MocoSolver* is packed in a *MocoStudy* (See Figure 13), which can be written to and loaded from XML files. Furthermore, the *MocoSolution* class contains utilities for plotting and visualizing a study's solution.

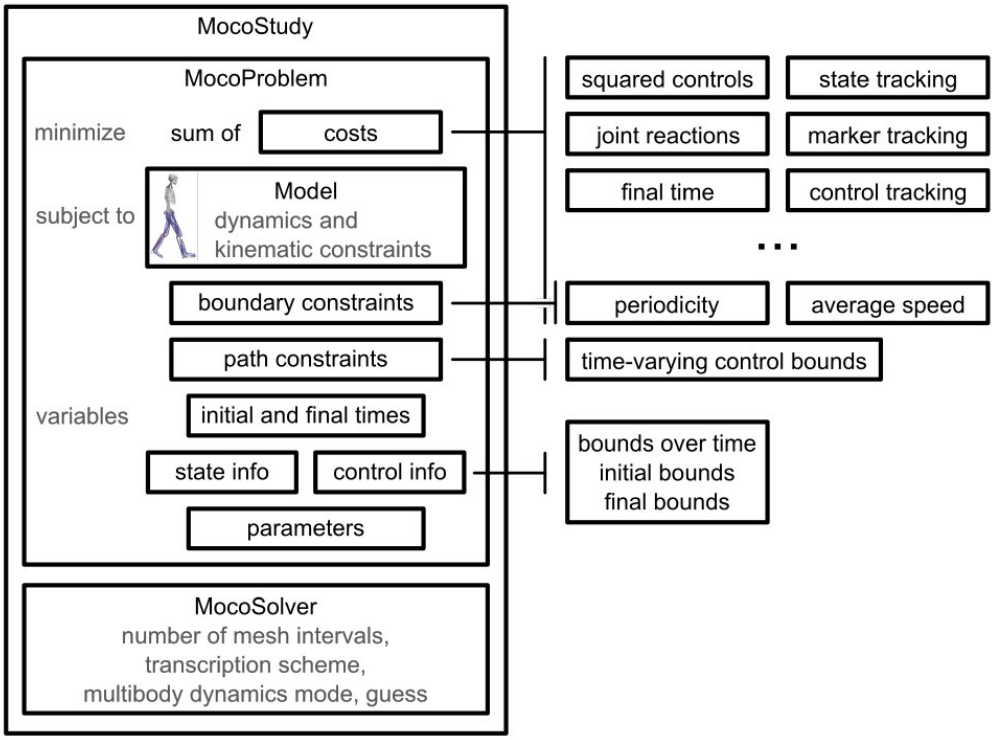

Figure 13: Overview of *MocoStudy*. Moco can solve custom optimal control problems using a library of cost, boundary constraint, and path constraint modules.[13]

Defining problems with *MocoProblem*

The *MocoProblem* formulation contains the following elements:

- **Cost terms.** By appending to the *MocoProblem* an instance of the class associated with the desired goal and its cost, a sum of weighted goals will be minimized. For instance, some goals can be: control effort (its class is *MocoControlGoal*), deviation from an observed motion, joint reaction loads or the duration of a motion.

- **Multibody dynamics, muscle dynamics and kinematic constraints.** Moco uses OpenSim *Models* to obtain the system multibody dynamics, auxiliary dynamics (for example the muscle activation dynamics and tendon compliance), and kinematic constraints.

- **Boundary constraints.** The average speed, symetry or periodicity can be defined with constraints relating initial and final states.

- **Path constraints.** Any function of time can be constrained to lie in a specified range over the motion.

- **Parameter optimization.** Model properties can be optimized, such as body's mass, muscle's optimal fiber length or an exoskeleton's stiffness.

- **Bounds on variables.** The values of the states, controls, initial and final time can be limited as well.

The modules of a *MocoProblem* can be combined in different ways, for example in a dynamically constrained inverse kinematics. In this case, the goal would be to minimize the error between experimental and model marker positions (marker tracking) and control effort while obeying multibody dynamics. The optimized variables would be generalized coordinates, speeds, and forces (See more examples in [13]).

MocoProblem describes the optimization problem in Equation 3, which consists of a summation of cost terms J_j multiplied by their weights w_j that depend on time-dependent states $x(t)$ and controls $u(t)$. The problem is constrained to the system dynamics $\dot{x}$, the path constraints $b(x, u)$, and the boundary conditions $c(x_0, x1)$. The cost functional is the sum of the endpoint cost and the continuous action (Equation 4). There are several goals available in Moco that can be used in the cost functional or as endpoint constraints. Some cost functionals are shown in Equation 5: the muscle effort cost, where w_i is the muscle weight and a_i is the muscle activation; the tracking "distance", where x_{exp} are the states of the experimental data; or the kinematics-based cost, where q are the system coordinates.

$$\begin{aligned} &\min_{x,u} \sum_j w_j J_j(x,u) \\ &\dot{x} = f(x,u), \quad b(x,u) \geq 0, \quad c\left(x_0, x_1\right) = 0 \end{aligned} \tag{3}$$

$$J_j(x,u) = \phi\left(x_0, t_0, x_1, t_1\right) + \int_{t_0}^{t_1} \mathcal{L}(x,u)\mathrm{d}t \tag{4}$$

$$\begin{aligned} J_{muscles} &= \sum w_i \int_{t_0}^{t_1} a_i^p \, \mathrm{d}t \\ J_{tracking} &= \int_{t_0}^{t_1} \left\| x - x_{\mathrm{exp}} \right\| \mathrm{d}t \\ J_{kinem} &= \int_{t_0}^{t_1} \mathcal{L}(q, \dot{q}, \ddot{q}, \dddot{q}, \ldots)\mathrm{d}t \end{aligned} \tag{5}$$

Solving problems with *MocoSolver*

As previously explained, the details of solving the optimal control problem are summarized in *MocoSolver*. *MocoSolver* uses the CasADi library to transcribe the continuous optimal control problem defined by *MocoProblem* into a finite dimensional nonlinear program, and it is solved with well-established gradient-based nonlinear program solvers such as OPOPT and SNOPT (For a better understanding, consult [13]).

Solving a *MocoStudy* yields a *MocoSolution*, which is a subclass of *MocoTrajectory* and allows easy access to the values of all the variables at any iteration during the optimization. In order to solve the *MocoStudy*, an initial guess can be provided using *MocoTrajectory* class, and the solution from one problem can be used as the initial guess for the following one (Figure 14).

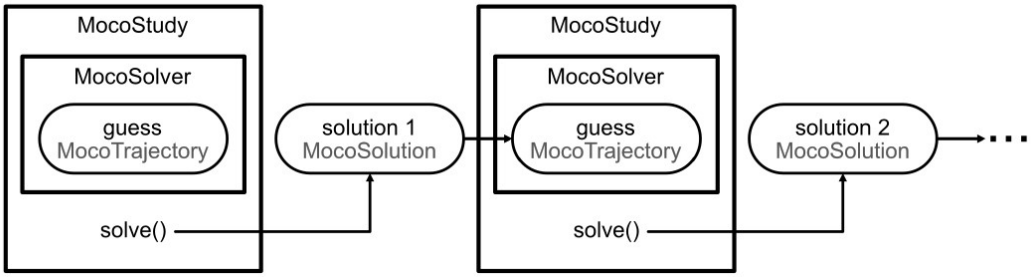

Figure 14: How the *MocoSolutions* can be used as the initial guess for the following study [13].

Once the problem is solved, Moco also provides the tools to visualize the solution as an animation, plot the state and controls of the trajectories, or even compute quantities from the solution.

Tools for standard problems

There are two tools in Moco developed to easily solve standard problems: *MocoInverse* and *MocoTrack*. The *MocoInverse* tool determines the controls (muscle activation or actuators) which minimize the distance to the prescribed motion, and it is useful for when an experimental motion should be followed. Whereas the *MocoTrack*, which is the tool used in this thesis, determines the controls which minimize the errors between the predicted motion and the reference motion. *MocoTrack* is useful for predicting deviations from motion data, for example in predicting kinematic adaptations to an exoskeleton or another device, as in this thesis.

Both these tools allow the use of contact models [4], as well as the application of external forces to the model. The application of measured external forces to the model (also known as ground-foot forces) requires the introduction of non-physiological "residual" actuators to resolve inconsistencies between the measured forces, measured kinematics and mass properties. As it is shown in the Figure 15, the only required inputs are the OpenSim model and the motion data (marker trajectories and external forces) and the previously mentioned settings in its *MocoStudy*.

[4]Contact models allow simulating the reaction forces and moments of the model with surfaces. The foot-ground contact modelling, for instance, enables to compute the ground reaction forces (GRF) and its moments.

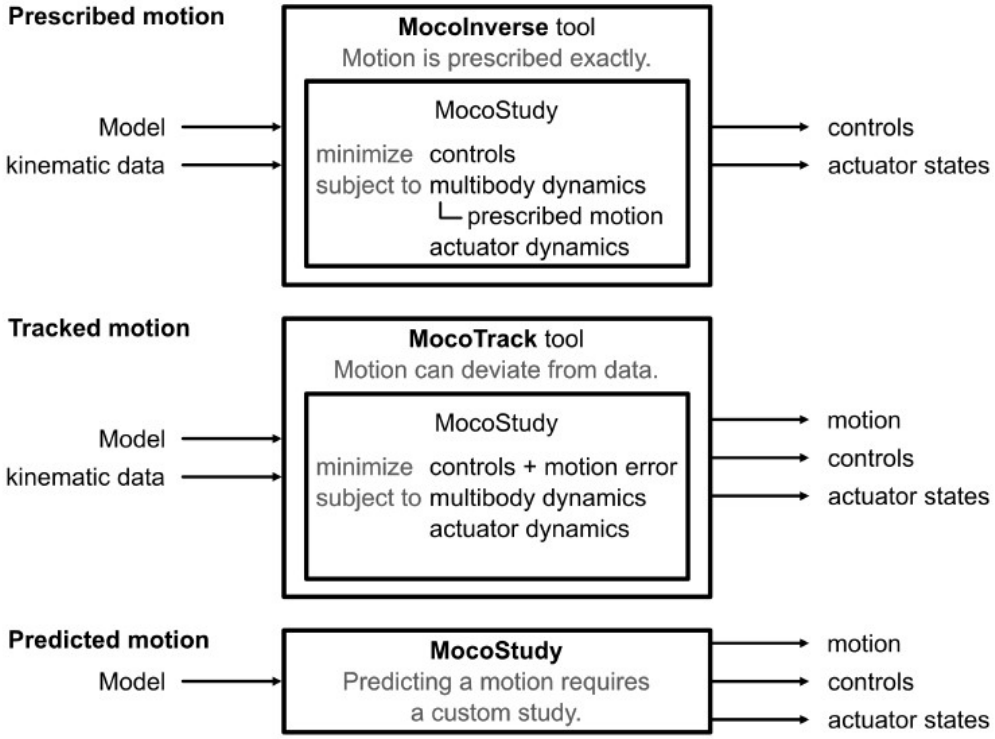

Figure 15: Solving prescribed motion, tracked motion, predicted motion problems and the Moco tool that each of these motions require. In order to predict a motion, which is a very common application in Moco, there is not a standardized tool. [13]

2.3 Lower limb passive assistive devices

As a part of the theoretical background, research on lower limb passive assistive devices is carried out with the objective of getting some inspiration for the design of the device. Two of the studies that have been found will be briefly explained in the following text.

2.3.1 Multidimensional springs system that can replace the muscle's torque during gait

ExoNET is a multidimensional springs system that can replace the muscle's torque during gait, and therefore decrease the metabolic cost of walking. The device is based on change of moment arm to control the generated torque: by moving the attaching point of the elastic elements at different positions with respect to the joint center of rotation, different torque fields can be generated. Because the anatomy of the human body is used as a rigid link, the need for a rigid skeleton is overcome. In Figure 16 a schematic model of the ExoNET for the right leg is shown. Each exotendon exerts a pulling tension T (represented as an arrow), blue for the hip exotendon, green for the knee exotendon and orange for the hip and knee exotendon. L1 is the distance between the hip and the knee, L2 is the distance between the knee and the ankle, ϕ_1 is the angle between L1 and the vertical, ϕ_2 is the angle between L1 and L2, r is the distance between the center of rotation (CoR) and the point where the exotendon is inserted, θ is the angle between r and the vertical. This device is user-friendly, customizable, safe, inexpensive and capable of

providing assistive torques to patients with motor deficits [35].

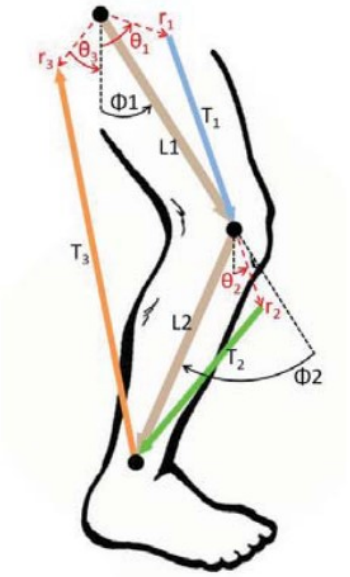

Figure 16: Schematic model of the ExoNET for the right leg.

2.3.2 Lightweight unpowered exoskeleton that reduces the energy cost of human walking

The hypothesis underpinning the device developed by Collins et al. [36] is that muscles consume metabolic energy to perform positive work, but they also use metabolic energy to produce force isometrically and to perform negative work, thus wasting energy. They designed a lightweight unpowered exoskeleton that provides some functions of the calf muscles and tendons during walking, but uses more efficient structures for those tasks. It has a spring in parallel with the Achilles tendon connected to the leg using a lightweight composite frame with a lever about the ankle joint, and a mechanical clutch in parallel with the calf muscles which engages the spring when the foot is on the ground and disengages it to allow free motion when the foot is in the air (see Figure 17). In the experiments they carried out with the device, it was demonstrated that the exoskeleton did not change the ankle joint ankles, and when the moderate-stiffness springs were used in the exoskeleton the human metabolic energy consumption was reduced.

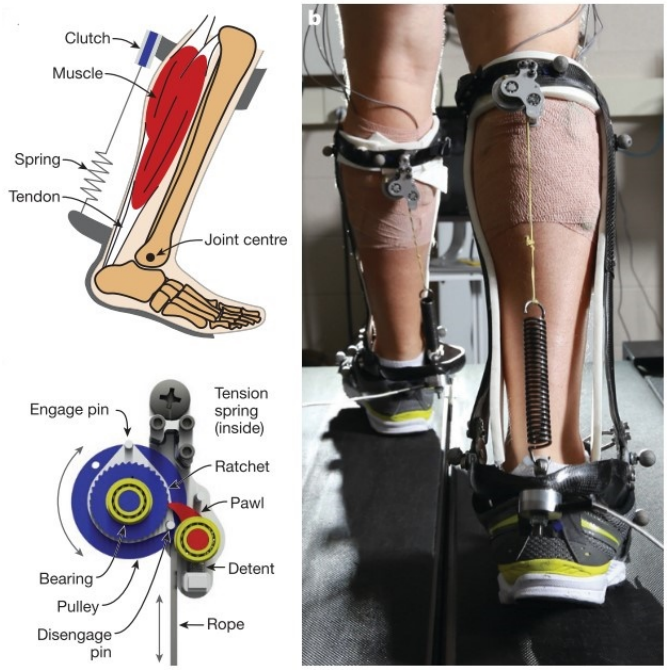

Figure 17: Unpowered exoskeleton design from Collins et al. study.

3 Methodology

The developed models, data, scripts, and results of this thesis have been worked from the BIOMEC GitHub's repository, which has allowed to share and benefit from previous research and development.

3.1 Lower limb musculoskeletal model

The complexity and accuracy of the musculoskeletal model needs to be chosen depending on the intended function. For this thesis, the model selected is *gait10dof18musc*[5], which is focused on the lower extremity, and originally has ten degrees of freedoms and eighteen muscles. The simplicity of the model allows faster simulations and optimizations, and has proved to be suitable for a first approach to the muscle dystrophy modelling. Some joints in the model were modified, thus adding more degrees of freedom, which allowed the model to fit better with the experimental data and to reproduce the movement more accurately.

3.1.1 Description of the model

The model has a total of twelve rigid bodies. The torso, the pelvis, and two legs consisting of femur, tibia, talus calcaneus and toes. The pelvis is the base segment of the model and has 3 DOF with respect to the ground associated with the pelvis tilt and displacements on the $x-$ and $y-axis$. The other segments are connected to the pelvis, and the motion of each segment is parametrized by joint coordinates relative to their parent segment. The torso segment includes the skull, spine and chest, and it has 1 DOF with respect to the pelvis associated with the lumbar extension/flexion. The femurs (right and left) have 1 DOF with respect to the pelvis, which is associated with the hip flexion/extension movement. The tibias have 1 DOF with respect to the femurs, associated with the knee extension/flexion. Each foot has three segments, the talus, calcaneus and toes, and 1 DOF with respect to the tibia associated with the plantarflexion/dorsiflexion movement. In Figure 18, pictures of the model.

With regard to the muscles, the model has eighteen muscles and at least one of them is representative of each group of movements of the joints in the sagittal plane [6]. The muscles in the model are symmetric, which means that for each muscle, there is one on the right side and one on the left side. For the hip flexion, the model has the **iliopsoas** muscles; for the hip extension, the **gluteus maximus** and the **biceps femoris**; for the knee flexion, the **hamstrings** and the biceps femoris; for the knee extension, the **vastus intermedius** and the **rectus femoris**; for the dorsiflexion, the **tibialis anterior**; and for the plantarflexion, the **gastrocnemius** and the **soleus**.

[5] This model is included with the OpenSim distribution, and it is supported by the OpenSim team.

[6] The sagittal or longitudinal plane is an anatomical plane which divides the body into right and left parts. Therefore, joint movements in the sagittal plane are flexion and extension only, no rotations or abduction movements.

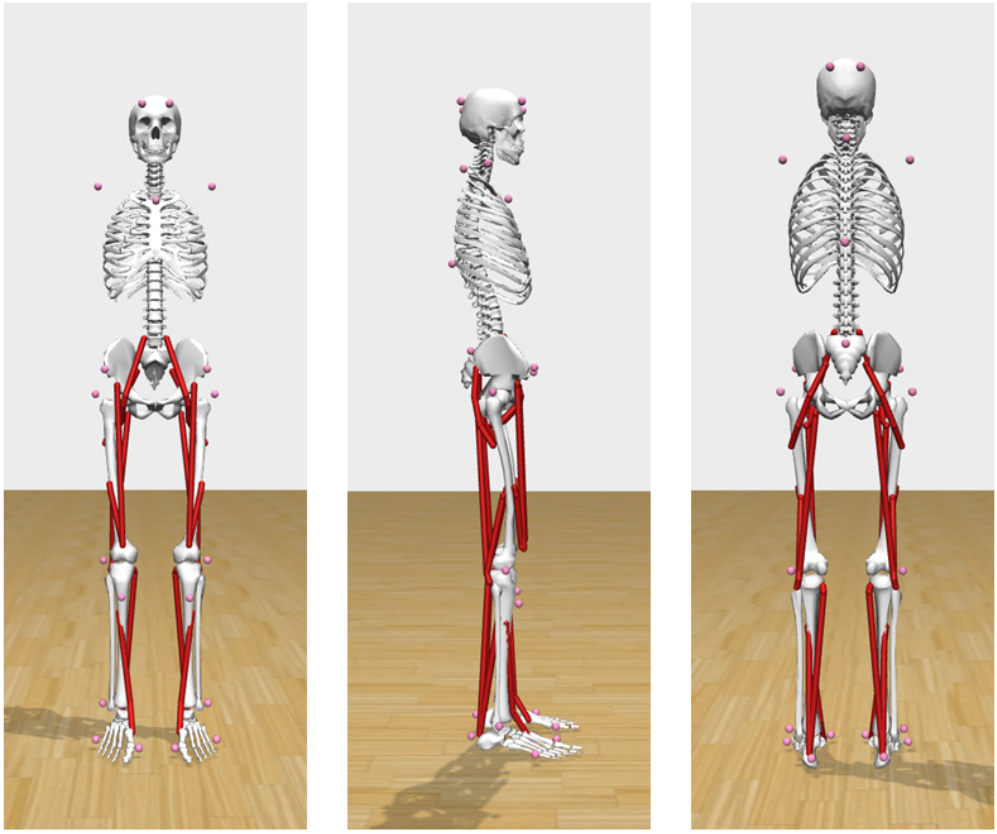

Figure 18: Front coronal, sagittal and back coronal planes of the model.

3.1.2 Modifications and scaling of the model

Although the purpose of the thesis is to make two-dimensions simulations, 4 DOF had to be introduced in the model in order to fit to the experimental data. The movements of rotation and displacement in the $z-axis$ were introduced in the pelvis, and the adduction/abduction of the femurs with respect to the pelvis as well. Additionally, it was introduced 1 DOF in each foot to allow the movement of the toes with respect to the calcaneus. Since the original model does not have these DOF, and therefore it is not able to reproduce any of these movements, a reserve actuator needs to be added in each new coordinate. Reserve actuators apply a generalized force in the direction of the generalized coordinate to which they are added, for example in the pelvis one reserve actuator will apply force in the $z-axis$ and another one will apply torque in the $y-axis$ (pelvis rotation).

In order to adapt the model, which originally represented an adult that is about 1.80 meters tall and has a mass of 75.16 kilograms, to the size and properties of children, the scaling tool in OpenSim was used. This tool, used directly from the GUI of the program, allows to adapt the model with the reference data it is given. In this case, two models were scaled using the data from the Exorapi Project, one for the child with DMD and one for the healthy child, both

nine years old (See Table 1). The scaling method in OpenSim involves two different actions: the registration of the markers placed on the generic model to match the locations of the new subject, and the scaling of the physical dimensions. Thus, in order to get an accurate scaling, the markers need to be placed correctly. In this case, the markers in the musculoskeletal model were placed manually through the OpenSim GUI and based on how they were placed in the Exorapi Project study from which the data was obtained (See Figure 19). Once the markers are placed correctly, the scaling tool calculates the scale factor that needs to be applied in each body in order to match the distance between the markers from the real data, and also the weight each body has in the new model. Therefore, after using the scaling tool, the model is anthropologically scaled and adapted to the data that is going to be used in the next steps.

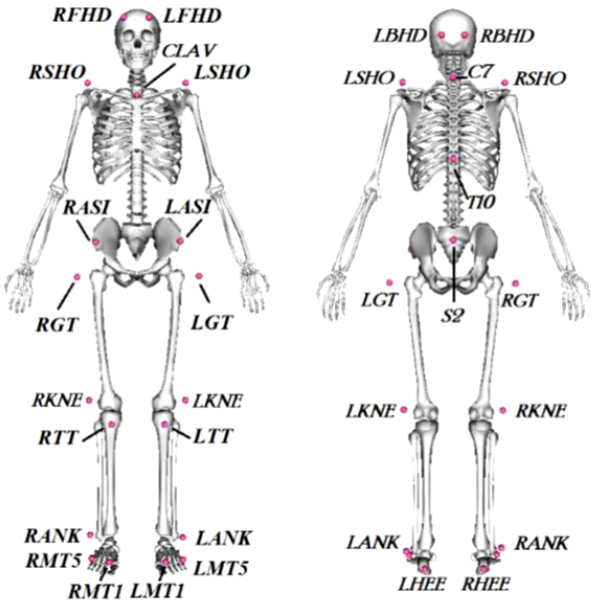

Figure 19: Markers placement from the Exorapi Project [14].

The last part of the scaling is the modification of the maximum isometric force [7], which has to be conducted directly in Matlab, given that the scaling tool does not modify the maximum isometric force of the muscles in the model. The chosen magnitude for the scaling of the maximum isometric force is calculated with the formula 6, and the muscle force scaling factors can be found in the Table 1.

$$forceScale = massScale \cdot heightScale \tag{6}$$

[7]The force in a muscle can be generated from four types of contractions: isotonic, concentric, eccentric and isometric. The isometric contractions generate force without changing the length of the muscle.

Model	Height [cm]	Mass [kg]	Height scale [-]	Mass scale [-]	Force scale [-]
gait10dof18musc	180	75.1646	1	1	1
DMD	127.5	35.6	0.7083	0.4736	0.3355
CONTROL	138	29.5	0.7667	0.3925	0.3010

Table 1: Characteristics of the data that was used for the models.

3.2 Data processing

In order to proceed with the tracking of the movement in Moco, the experimental data needs to be processed. With the model described in the previous section and the experimental data of the markers, an Inverse Kinematics is carried out directly in the OpenSim GUI with the Inverse Kinematics tool.

Kinematics is the study of motion without considering the forces and moments that produce it. Therefore, the purpose of inverse kinematics (IK) is to estimate the joint angles and displacement of a given musculoskeletal model from experimental data (Figure 20). In order to do so, OpenSim computes a set of joint angles that position the model in a configuration that matches the experimental kinematics for each time step in the recorded data. To obtain the "best match" for the positions, OpenSim solves a weighted least squares optimization problem with the goal of minimizing the distance between the experimental marker and the corresponding model marker (also called the *Marker error*). Each marker can be given a different weight depending on how strongly that marker's error should be minimized. In this thesis, all the markers were given the default weight for the IK.

Figure 20: Inverse Kinematics overview.

Focusing on the mathematical formula OpenSim uses to calculate the "best match" for every position, OpenSim solves for a vector of generalized coordinates, $\mathbf{q}$, that minimizes the weighted sum of marker errors and is expressed as in the Formula 7. The vector of generalized coordinates ($\mathbf{q}$) is usually the joint angles or displacements.

$$\min_{q} \left[\sum_{i \in \text{ markers}} w_i \left\| \mathbf{x}_i^{\text{exp}} - \mathbf{x}_i(\mathbf{q}) \right\|^2 \right] \tag{7}$$

In Formula 7, $\mathbf{q}$ is the vector of generalized coordinates, $\mathbf{x}_i^{\text{exp}}$ is the position of *experimental marker* i, $\mathbf{x}_i(\mathbf{q})$ is the position of the corresponding *model marker* i (which depends on q), and w_i is the weight associated with marker i.

As a result of the IK, a trajectory file with the coordinates of each joint in each time step is created. This trajectory, is used as an initial guess for the next step: the tracking of the movement.

In addition to the marker data, the experimental data also includes data from the force plates of each. The force plaques' data allows defining the initial and final times, and also indicate the gait cycle for each patient. In this case, the force plaques do not include the whole gait cycle, only from the opposite toe off to the next initial contact (10% - 100% GC).

3.3 Tracking of the movement

The tool that has been used is the *MocoTrack* (See Chapter 2.2.2 for more information about the available tools). The *MocoTrack* approach allows to explain how a change in a system parameter or optimization criteria affects the optimal kinematics in the system by adding a cost term that computes the error between experimental data and the associated model quantities. Two trackings were carried out, one for the control model and one for the DMD model, each of it with their respective trajectories and bound. In the following text, the *MocoStudy* definition and *MocoSolution* of this *MocoTrack* will be explained.

3.3.1 Problem definition

The *MocoStudy* is decapsulated in two parts, the *MocoProblem* and the *MocoSolver* (see Figure 13). The parameters that have been defined in the *MocoProblem* will be explained below.

Cost terms

As explained in Chapter 2.2.2, multiple goals can be added to the cost function with their associated weights, and the software will solve the problem for both a motion and muscle (or other actuator) controls that minimize the error with an observed motion in addition to the other costs.

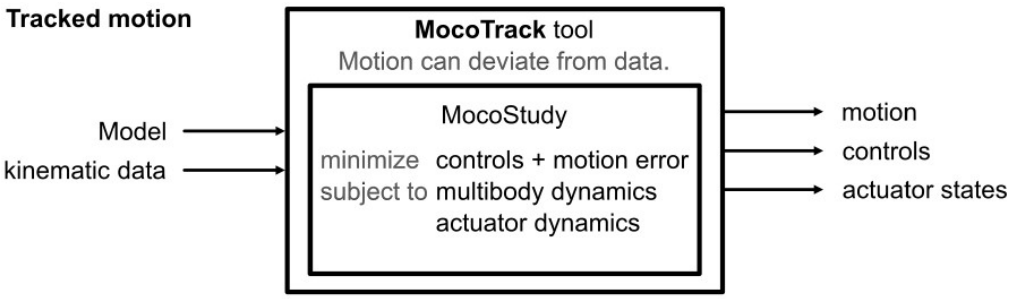

Figure 21: *MocoTrack* tool. [13]

For instance, the goals that were set for the tracking of the movement were:

- **State tracking goal.** In order to get the most similar solution to the reference given (which is the corresponding IK for each tracking), this goal is set. The squared difference between a state variable value and a reference state variable value, summed over the state variables for which a reference is provided, and integrated over the phase. Weights can be set for each coordinate, which allows emphasising the accuracy of the movement regarding the reference in those coordinates. The coordinates in the pelvis and feet were set to 1, and the ones in the hip and knee were set to 0.1.

- **Muscle effort goal.** This goal helps minimize the activation of the muscles (controls) in order to simulate better the human body. It minimizes the sum of the absolute value of the controls raised to a given exponent, integrated over the phase.

- **Initial activation goal.** It is necessary to add this goal to avoid an excessively high activation at the beginning of the problem. Thanks to this endpoint constraint goal, the initial excitations and activations are the same.

- **Reserve actuators goal.** In order to solve the problem, a reserve actuator[8] is added to every coordinate of the model that will activate in case the muscles cannot reproduce the movement. This goal is implemented to reduce these activations, so that the reserve actuators only work when it is necessary. The goal works the same way as the muscle effort goal.

Multibody dynamics, muscle dynamics and kinematic constraints

The multibody dynamics, muscle dynamics and kinematic constraints are obtained from the model defined in OpenSim. In order to solve the problem, the muscles in the models need to be changed to *DeGrooteFregly2016Muscle*. Additionally, and as it has been mentioned previously, **reserve actuators** are added to all the coordinates in the model.

As a way to model muscular dystrophy in the DMD model, the isometric force is scaled. This procedure will be explained at length in the next chapter (3.4).

The corresponding **time bounds**, along with the **external forces**, explained in the previous chapter, are set in each *MocoStudy*.

[8] Reserve actuators apply a generalized force in the direction of the generalized coordinate to which they are added when the muscle is not able to complete the movement by itself. They are three main reasons why reserve actuators are added to the model when solving an optimization: (a) the muscles are not strong enough to achieve the required net joint moments, (b) the net joint moments change more rapidly than activation and deactivation time constants allow, and (c) the filtering of the data causes unrealistic desired net joint moments [12]

Bounds on variables

Additionally, bounds on some variables are set in order to help the optimization. The bounds are set on the initial value and the range of motion, and the values were defined from the reference data (the IK) with additional margin for each model.

3.3.2 Solver definition

Below, the *MocoSolver* parameters that have been defined for the problem:

- To define the **number of mesh intervals**, the following formula was applied:

$$SolverMeshIntervals = round\left(100 \cdot (t_f - t_0)\right) \tag{8}$$

- The **maximum number of iterations** for optimisation is set to 1000, which is a sufficiently large number for Moco to find a solution without exceeding it.
- The **optimal convergence and constraint tolerance** is set to 0.01.
- The **initial guess file** is the IK file for each model. This is the same file that is used as a reference for the movement.

The solver used is *MocoCasADiSolver*, with the Hermite-Simpson transcription scheme, implicit multibody dynamics mode (which means the multibody dynamics are expressed as implicit differential equations), random sparsity pattern of derivatives and the forward finite difference scheme to calculate problem derivatives. More information about these parameters can be found in [12].

3.3.3 Solution

When the problem is solved, a *MocoSolution* is obtained, which is a subclass of *MocoTrajectory* that allows to visualize the solution as an animation, plot of the states and control trajectories or compute quantities from the solution. From each tracking, plots and quantities of the coordinates, muscle, and reserve actuations were obtained and will be disscussed in Chapter 4.

3.4 DMD modelling

Although it may seem logical to use the *DMD* model to design the device, considering the approach used in this thesis, it is not possible to do so. The *MocoTrack* approach allows explaining how a change in a system parameter, such as modifications in the model, affects the optimal kinematics in the system. Therefore, by modifying the model with the objective of modelling muscular dystrophy, some parameters in the solution will be different in respect to the unmodified model. The hypothesis that has been put forward is that if the maximal isometric force is

decreased (as it is in patients with DMD) and the muscle excitations are limited (thus making them unable to exert force), the reserve actuators will be forced to perform. Subsequently, the performance of the actuators can be analysed in order to design the device.

3.4.1 Decreasing of the maximal isometric force

As explained in Chapter 2.1, the maximal isometric force in the muscles of children with DMD is lower than in healthy children. To quantify this difference and apply it in the model, a force scaling is calculated with the values from the Biomechanical analysis carried out in the Exorapi Project [14]. One of the tests carried out in the study was the muscle strength test using a hand held dynamometer, which measured the passive muscle strength of the muscular groups responsible for the flexion/extension of the hip, knees, and feet. Since the models and data used in this thesis are specific for two patients, the values of the dynamometer are also specific for each patient. In Table 2, the normalized values of the aforementioned test are shown.

	Normalized forces [N/kg]					
Patient	**HF**	**HE**	**KF**	**KE**	**AF**	**AE**
DMD	1.793	1.650	2.424	1.993	0.856	1.250
CONTROL	3.084	4.546	2.201	3.430	2.367	3.023

Table 2: Forces normalized by weight for each patient in the study. HF stands for Hip Flexion, HE for Hip Extension, KF for Knee Flexion, KE for Knee Extension, AF for Ankle Flexion (also known as dorsiflexion) and AE for Ankle Extension (also known as plantarflexion).

In order to find a suitable force scaling for the models in order to model the dystrophy, two methods were applied:

1. To calculate the force scaling for the *CONTROL* model, the force of the control has been taken as the base from which to scale. That is, the muscle force of the healthy patient has been assumed to be the 100% of the model force, and it has been scaled in relation to that force using the following formula for each group of muscles:

$$Normalized\ scale = \frac{DMD\ Normalized\ force}{CONTROL\ Normalized\ force} \tag{9}$$

2. To calculate the force scaling for the *DMD* model, which has been used in Chapter 3.3, a non-normalized scale is calculated for each group of muscles using the following formula:

$$Non-normalized\ scale = Normalized\ scale \cdot \frac{DMD\ weight}{CONTROL\ weight} \tag{10}$$

Since there is at least one muscle in the models that is responsible for each one of the movements, the force scaling was applied accordingly. The only muscle that needed a special scaling

	Force scales [-]					
Patient	**HF**	**HE**	**KF**	**KE**	**AF**	**AE**
Normalized scale	0.580	0.363	1.101	0.581	0.361	0.4135
Non-normalized scale	0.702	0.438	1.330	0.701	0.436	0.50

Table 3: Normalized and non-normalized force scales. The normalized scale is calculated with the formula 9 and the non-normalized scale with the formula 10.

factor is the biceps femoris because it is responsible for the hip extension and also the knee flexion. Therefore, the mean between the force scaling of these movements was calculated for each model and applied to the biceps femoris muscle.

3.4.2 Restriction of the muscle excitations

As explained in Chapter 2.1, the muscles of the lower limb hyper-activate as a compensatory strategy for the muscles' weakness. On the basis of this information, it is expected to see a hyper-activation in the most affected muscles of the model, but in order to be able to analyse it more easily and design a device to assist walking, the excitations of the muscles have been restricted. The restriction of the muscle excitations also endorses the idea of avoiding muscular fatigue in children with DMD.

By restricting the excitations to 0.5, it has been observed that the reserve actuators "activate" and perform the work the model by itself is not able to do. Since the reserve actuators apply a torque in the direction of the generalized coordinate they are applied to, it allows observing which movement needs more support. Therefore, the movement that needs more support from the reserve actuator is the one that will be analysed in order to design the spring. The ultimate goal, which will be explained in the next chapter, is for the designed device to be able to reproduce the force (or in this case, the torque) that the reserve actuator makes, thus avoiding the hyper-activation of the muscles while assisting the model in the gait.

3.4.3 Tracking solution

After altering the *CONTROL* model, which will be referred to as the *WEAKENED* model from now on, another *MocoTrack* is carried out. The expected result is for the model to correctly reproduce the movement, but to observe some changes in the muscle activations and the performance of the reserve actuators. The problem definition is the same as before, except for the alterations carried out in the model. The plots and quantities of the solution's output will be discussed in Chapter 4.

3.5 Design of the device

With the results obtained from the *"WEAKENED" MocoTrack*, different analyses are carried out to determine the design of the most suitable device. The first step of the process is to decide in which joint the device will be placed based on where it is needed the most. As it is shown in Table 4 and Figure 22, the highest torque is performed by the reserve actuator in the **right hip**.

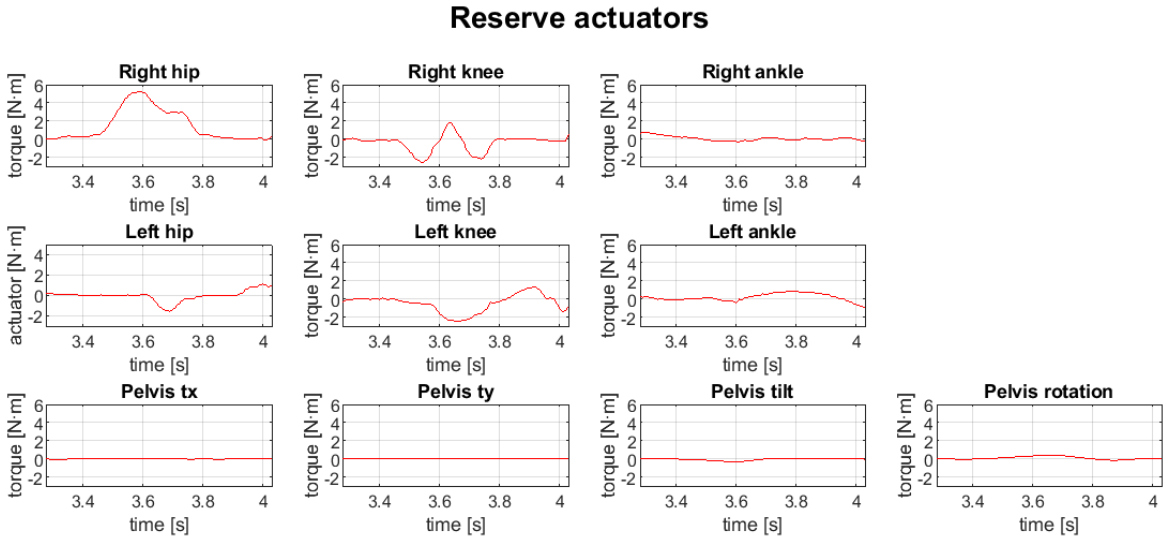

Figure 22: Reserve actuators' performance in the *WEAKENED* tracking. The highest torque is applied by the reserve actuator in the right hip.

Reserve Actuators	Mean [N·m]	Maximum [N·m]	Minimum [N·m]
Right hip	1.49974	5.19265	-0.13477
Left hip	-0.02885	1.13550	-1.53653
Right knee	-0.42316	1.80708	-2.58546
Left knee	-0.492405	1.35561	-2.41877
Right ankle	0.067546	0.77996	-0.31817
Left ankle	0.17276	0.86345	-0.95534
Pelvis tx	-0,01705	0,031465	-0,07788
Pelvis ty	-0,00206	0,007557	-0,01727
Pelvis tilt	-0,07028	0,032832	-0,31594

Table 4: Torque values of the reserve actuators in the *WEAKENED* tracking. The actuator with the highest torque is the one in the right hip.

In order to understand this behaviour, it is needed to observe the muscle activations, in this case the right muscles. In Figure 23, it can be observed how the right iliopsoas, responsible for the hip flexion, is at maximum activation for almost the whole gait cycle, and during the terminal stance and the pre-swing periods is when the right hip reserve actuator performs a high torque.

During this two periods, the right hip goes from an extended position to a more flexed position, which means that the right iliopsoas muscle is too weak to perform the hip flexion and needs help from the reserve actuator.

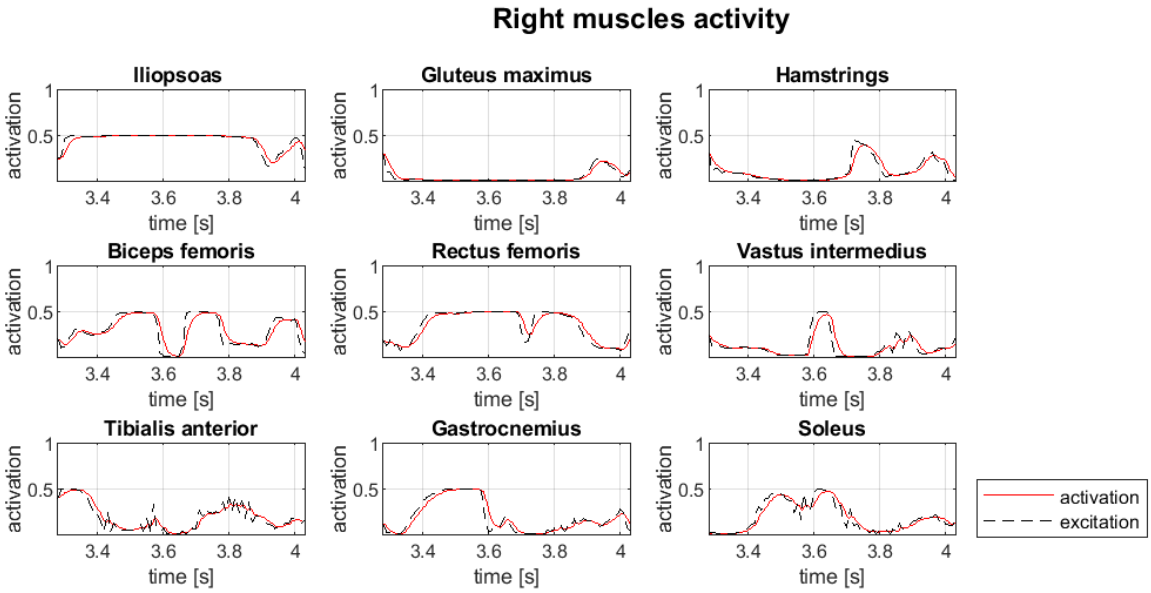

Figure 23: Right muscles activity of the *WEAKENED* tracking.

Once the joint in which the device will be placed has been decided, the performance of this joint's reserve actuator needs to be analysed. In order to simplify the design of the device, it has been decided to design a **linear torsional spring**, so first degree lineal regressions are used to obtain the parameters of the device from the function of torque versus angle of the right hip. In Equation 11, $M_{\text{rh}}^{\text{dev}}$ is the torque provided by the actuator in the right hip ([N·m]), k is the torsional stiffness ([N·m/rad]) and θ_{rh}^{0} is the right hip joint angle for which the moment of the spring is zero ([rad]).

$$M_{\text{rh}}^{\text{device}} = -k\left(\theta_{\text{rh}} - \theta_{\text{rh}}^{0}\right) \tag{11}$$

Three analyses have been carried out to obtain different parametrizations of the spring.

Lineal regression of the whole gait

The first analysis that has been performed considers the whole gait cycle, and it has been applied not only to the right hip reserve actuator but to all of them. This analysis allows verifying how accurate is the lineal regression for each reserve actuator, as it could be the case that the most active reserve activator cannot be parametrized by a first degree linear regression. In the Figure 24 it is shown the plot of the reserve actuator's torque versus the joint angle and the first degree lineal regression of each function. And in the Table 5 the parameters of these lineal regressions.

As expected, the linear regression at the right hip fits correctly, although some data seem to be deviated.

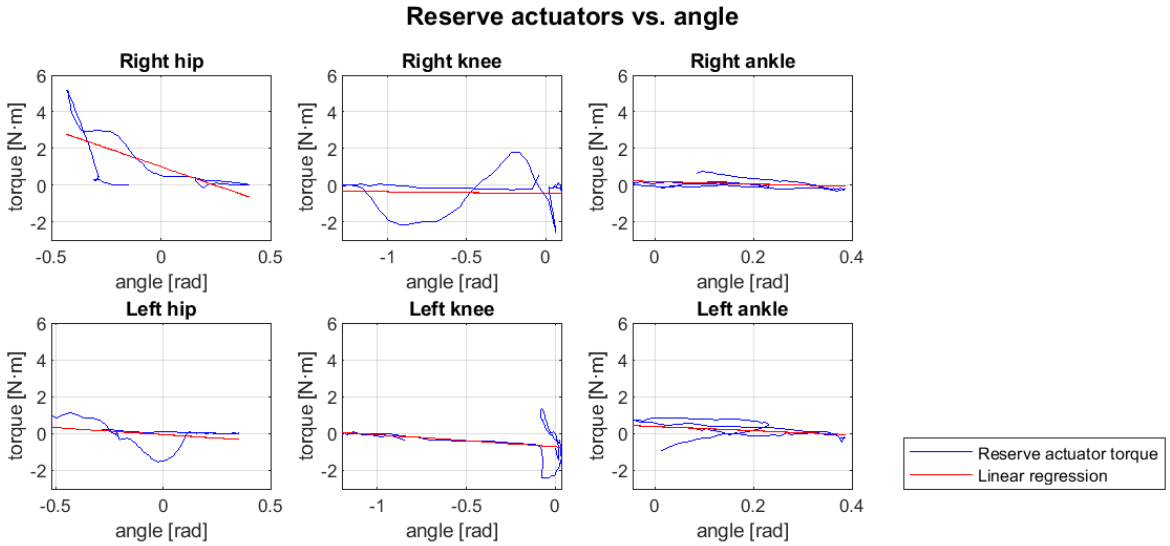

Figure 24: Plot of the reserve actuator's torque versus the joint angle for each joint and their respective lineal regressions. The blue line is the right hip reserve actuator's torque, and the red line is the obtained lineal regression.

Joint	$k\ [N \cdot m/rad]$	$M_0\ [N]$	$\theta_0\ [rad]$
Right Hip	4.1026	1.0062	0.24526
Left Hip	0.75411	-0.057134	-0.075763
Right Knee	0.10096	-0.46396	-5.00000
Left Knee	0.65029	-0.71473	-1.00000
Right Ankle	0.67067	0.19213	0.28647
Left Ankle	1.1255	0.38183	0.33925

Table 5: Parameters obtained from the first degree lineal regression for each reserve actuator. The row of the right hip reserve actuators is highlighted in yellow.

Lineal regression for each phase of the gait

In order to adjust the parametrization of the spring, the analysis is separated by phases of the gait, thus obtaining a lineal regression for each phase. The lineal regression of each phase is then compared with the lineal regression for the whole gait for the purpose of determining the phases that are more deviated.

In Figure 25 it can be observed the plots of the torque applied by the reserve actuator versus the angle of the right hip for each phase of the gait cycle, the lineal regression for each period and the lineal regression for the whole cycle. It can be observed that the range of data that is more

deviated from the lineal regression is in the midstance and terminal stance.

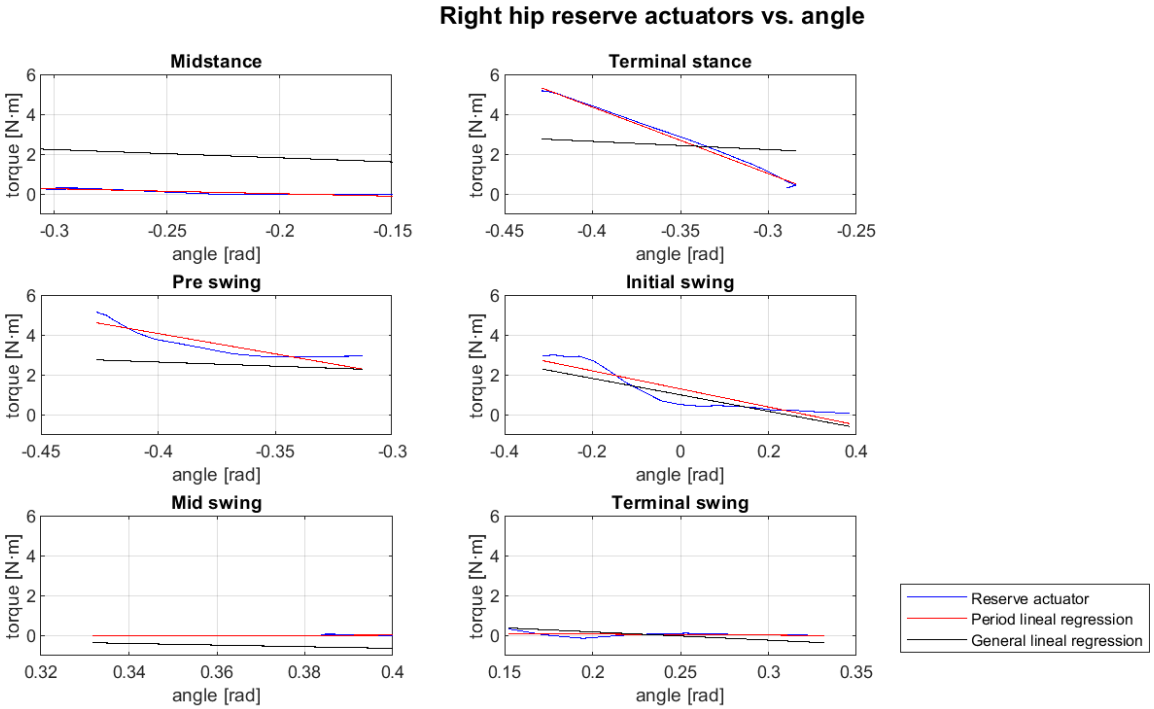

Figure 25: Plot of the right hip reserve actuator's torque versus the joint angle for each gait cycle phase. The blue line is the right hip reserve actuator's torque, the red line is the obtained lineal regression for each phase, and the black line is the lineal regression for the whole gait.

Lineal regression for some parts of the gait

The last approach for the parametrization of the device is based on not considering the data that deviate more from the general linear regression. From the previous analysis, it has been concluded that the phases with deviation are midstance and terminal stance, so a new lineal regression is carried out excluding the data from these phases. The results of this last lineal regression can be seen in Figure 26 and Table 6.

Range of the GC	$k\ [N \cdot m/rad]$	$M_0\ [N]$	$\theta_0\ [rad]$
50% to 100%	5.446	1.8997	0.34883

Table 6: Parameters obtained from the first degree lineal regression of the right hip reserve actuator's torque, from the 50% to the 100% of the gait cycle.

In conclusion, by excluding the data from those two phases, the lineal regression fits better than before.

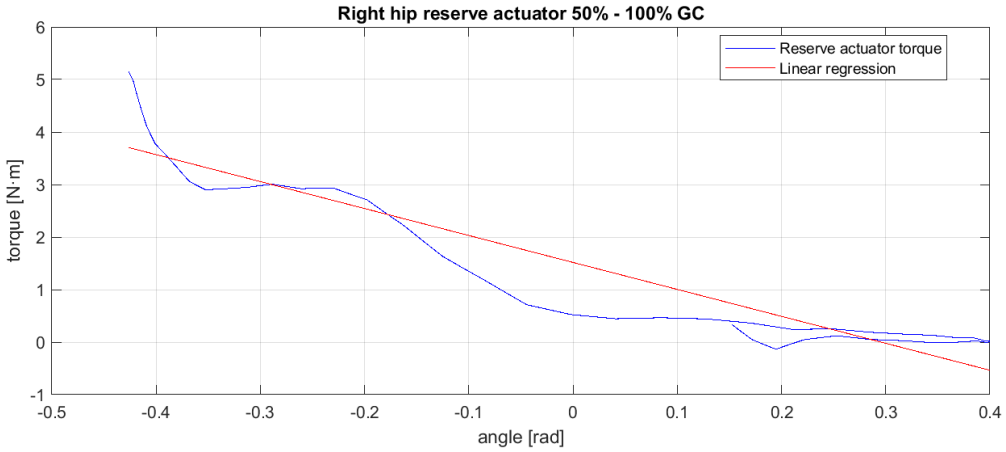

Figure 26: Lineal regression excluding the data from the midstance and terminal stance phases. The blue line is the right hip reserve actuator's torque, and the red line is the obtained lineal regression.

3.5.1 Designed devices and implementation

As a result of the previous analyses, three possible springs were designed and tested out. The The parameters of **Spring 1** were obtained from the lineal regression of the whole gait cycle, the parameters of **Spring 2** were obtained from excluding the data from the midstance and terminal stance, and the parameters of **Spring 3** have been designed as the average of the previous springs' parameters.

Names	$k\ [N \cdot m/rad]$	$M_0\ [N]$	$\theta_0\ [rad]$
SPRING 1	4.1026	1.0062	0.24526
SPRING 2	5.446	1.8997	0.34883
SPRING 3	4.7743	1.45295	0.297045

Table 7: Parameters of the three designed springs

In order to implement the device in the model, it is added in the *MocoStudy* as a *SpringGeneralizedForce*, which is a force that exerts a generalized force based on spring-like characteristics such as stiffness and viscosity. The spring is added in the right hip flexion with the defined parameters of stiffness (k), rest angle (θ_0), and a proportional dumpling of coefficient 10^{-3} to stabilize the simulation. With the addition of the spring in the model, the restriction in the excitations of the muscles is deleted so that the model represents a child with muscle dystrophy with the designed device.

3.5.2 Tracking solution

Three trackings are performed: one with each designed spring implemented. The *MocoStudy* definition is the same as in Chapter 3.3, except for the alterations carried out in the model. The obtained solutions will be analysed in Chapter 4.

4 Results and discussion

In this section, the plots and quantities of the coordinates, muscle, and reserve actuations obtained in each tracking will be exposed and analysed. The names of the subsections in this chapter match those in the previous chapter, e.g., in Chapter 4.1 the results from Chapter 3.3 will be exposed and analysed, and so on. As a final point, the limitations of the thesis will be discussed.

Because of the approach of *MocoTrack*, the values of the kinematic of the movement will be analysed in order to quantify the error between the solution and the reference. For this purpose, the **root-mean-square** (RMS) of each coordinate has been calculated with formula 12 where i is the coordinate in the model, n are the time steps in each tracking, x_i^{sol} is the value of the coordinate i in the solution and x_i^{ref} is the value of the coordinate i in the reference.

$$RMS_i = \sqrt{\frac{1}{n} \cdot \sum_n (x_i^{sol} - x_i^{ref})^2} \tag{12}$$

In order to quantify the RMS, the percentage with respect to the range of motion of the reference will be calculated for each coordinate, and it will be referred to as $\%RMS$. To analyse the controls in the model, that is, muscle activations and reserve actuators, graphics with the mean activations and mean torques will be used. The values of these parameters can be found in A.3.3, along with other information that has been obtained from the simulations.

4.1 Tracking of the movement

As shown in Figure 27, the $\%RMS$ values for almost all the coordinates are around 10% or lower. The highest values are in the pelvis displacement in the $y-axis$ (pelvis "ty" displacement) and in the pelvis tilt. This is probably because the contact forces are not properly aligned with the OpenSim axes, additionally to the error there might be in the location of the center of mass of the models, since they have been scaled but not calibrated.

As for the muscle activations (see Figure 28), a grater activation in the muscles has been found in the *DMD* tracking, thus matching the findings of other studies. The hypothesis is that the *DMD* model has to hyper-activate the muscles for two reasons: because the maximum isometric force of the muscles is lower (as it is in children with DMD), and also because the movement to reproduce is pathological and the model needs to do an extra effort.

In Figure 29 it can be observed that the values of the torque applied by the reserve actuators in these solutions are very low, which means the models were strong enough to reproduce the movement by themselves.

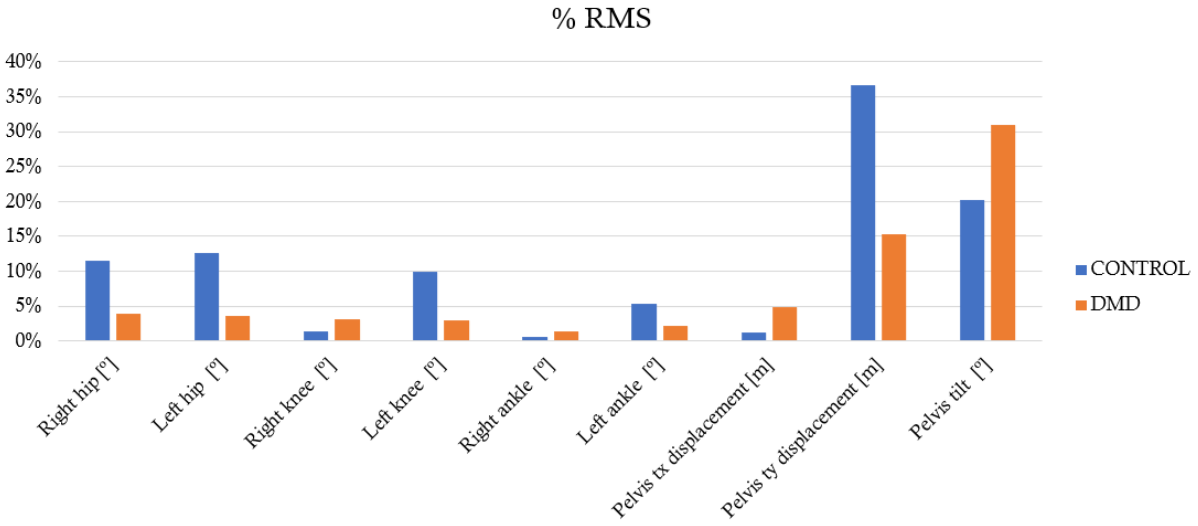

Figure 27: $\%RMS$ values of the trackings of *DMD* and *CONTROL* models.

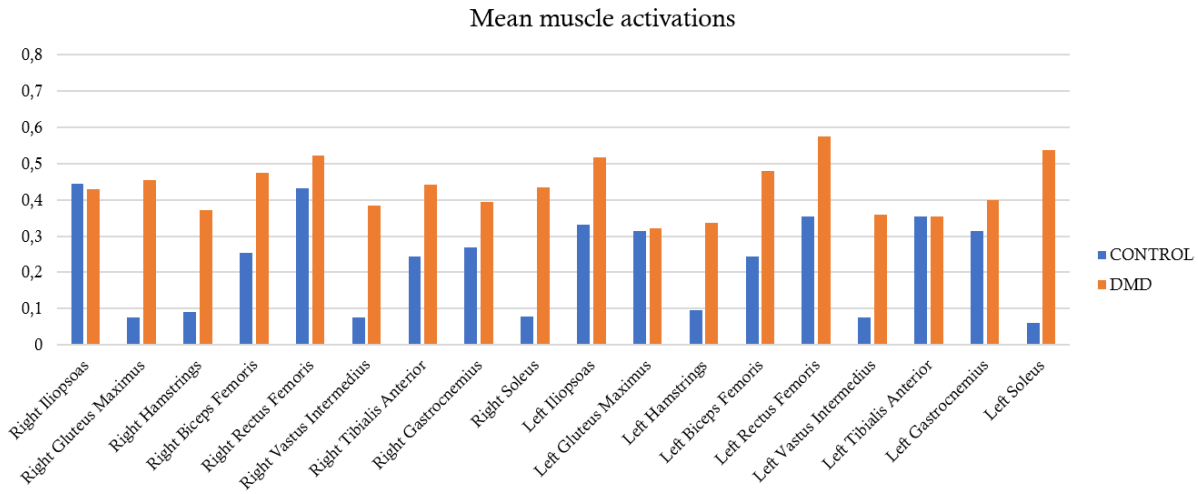

Figure 28: Mean muscle activations of the trackings of *DMD* and *CONTROL*.

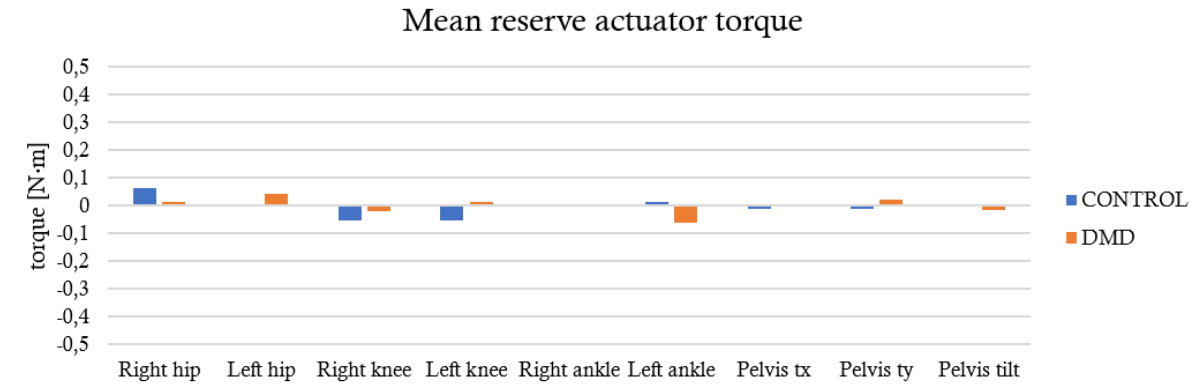

Figure 29: Mean reserve actuator torque in the *DMD* and *CONTROL* trackings.

To sum up, the tracking of the movement with both models is considered correct due to the low values of the $\%RMS$ and the reserve actuators. Additionally, the hypothesis of modelling muscular dystrophy through a reduction of maximal isometric force has been proved to be correct.

4.2 DMD modelling

As shown in Figure 30, the $\%RMS$ values are slightly higher in the *WEAKENED* solution than in the *CONTROL* one, which means that the tracking is less similar to the reference. This is probably because the actuators were responsible for reproducing some of the joint movements, thus creating a less similar to the reference.

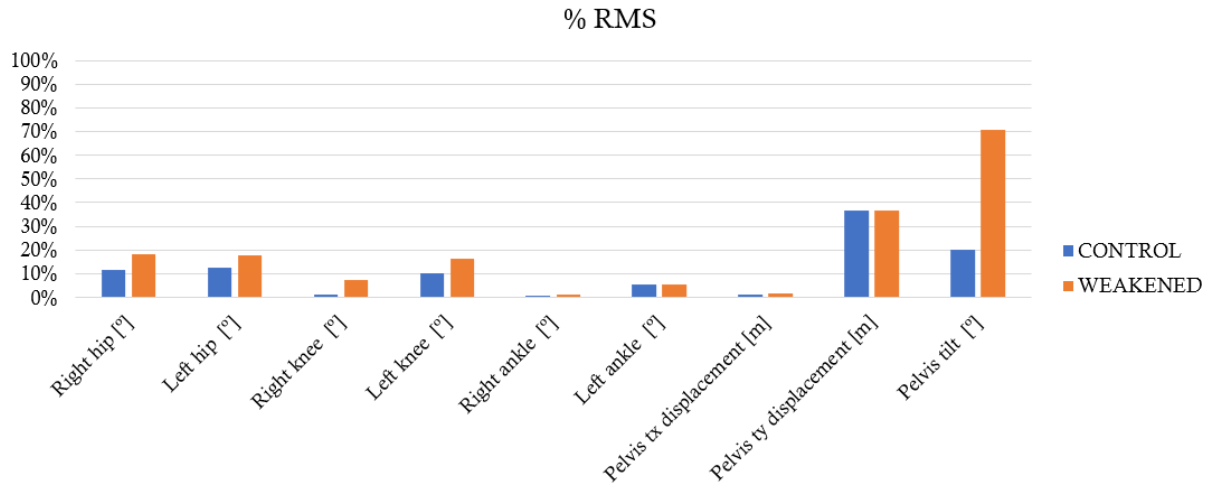

Figure 30: $\%RMS$ values of the trackings of *CONTROL* and *WEAKENED* models.

As shown in 31 In overall, the muscle activations are similar in the *WEAKENED* tracking with respect to the *CONTROL* one, although some muscles are more activated (e.g., soleus) or less activated (e.g., rectus femoris).

In Figure 32, there is a comparison of the means of the reserve actuators' torque of the *WEAKENED* and *CONTROL* tracking. It has been found that the right hip reserve actuator helps the right iliopsoas muscle in the hip flexion during the terminal stance and pre-swing periods (see Chapter 3.5).

4.3 Design of the device

The three simulations have almost the same $\%RMS$, which means that the obtained movements are equally different from the reference. When compared to the *CONTROL*, it is observed that the differences are notable only in the pelvis tilt.

As shown in Figure 34, the implementation of a spring in the model decreases the muscle activations to levels similar to the *CONTROL*. Focusing on the right iliopsoas, which was found to be the muscle that needs more assistance in the movement, the spring that reduces its activation

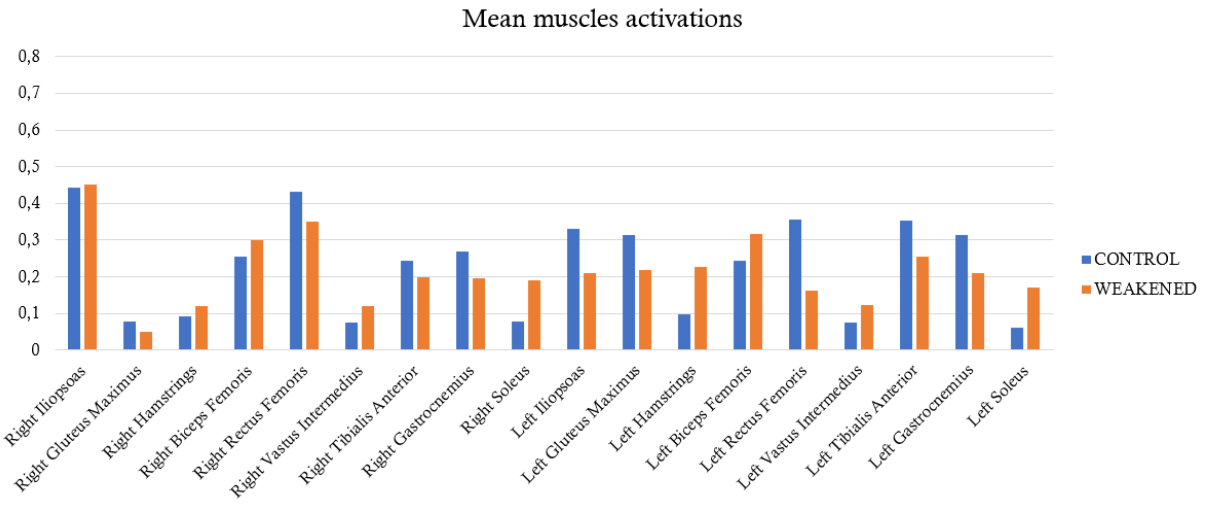

Figure 31: Mean values of the muscles activations in the *CONTROL* and *WEAKENED* trackings.

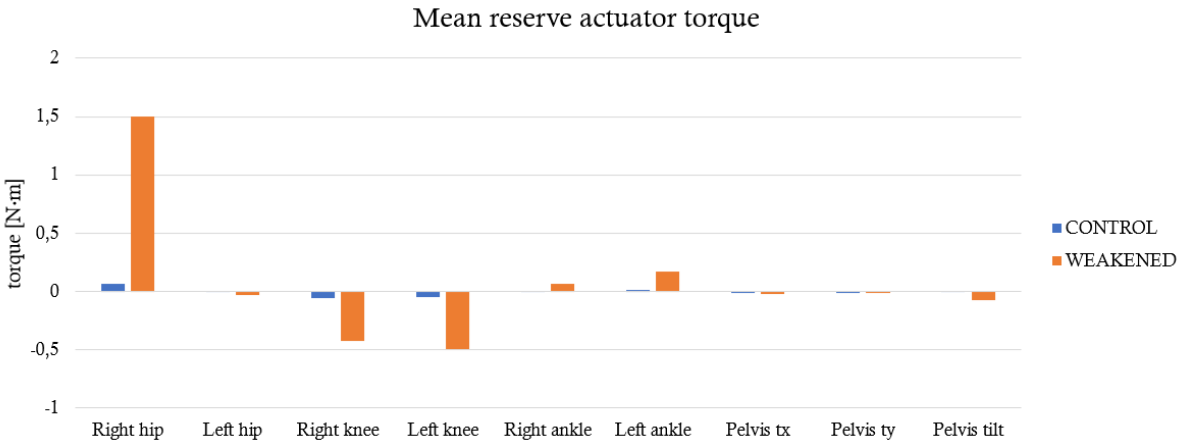

Figure 32: Torques applied by the reserve actuators in the *CONTROL* and *WEAKENED* trackings.

the most is the *SPRING 2*. It is worth noting the behaviour of the left biceps femoris and the left rectus femoris. On one hand, the left biceps femoris, responsible for the left hip extension, shows a higher activation when a spring is implemented than in the *CONTROL*. On the other hand, the left rectus femoris, responsible for the left hip flexion and knee extension, shows a lower activation when a spring is implemented. It is believed that the spring implemented provokes an abrupter hip flexion movement, thus forcing the left biceps femoris to hyper-activate in order to maintain the left hip extension.

In Figure 35 the difference between the muscle activations in the *CONTROL* and *SPRING 2* trackings can be observed in more detail. The activations in the model with *SPRING 2* are, in general, similar to the ones in *CONTROL*, which is considered to be a very positive result considering that reducing the hyper-activation of the muscles was one of the objectives of the design of the device. However, the hyper-activation of the left biceps femoris is considered to

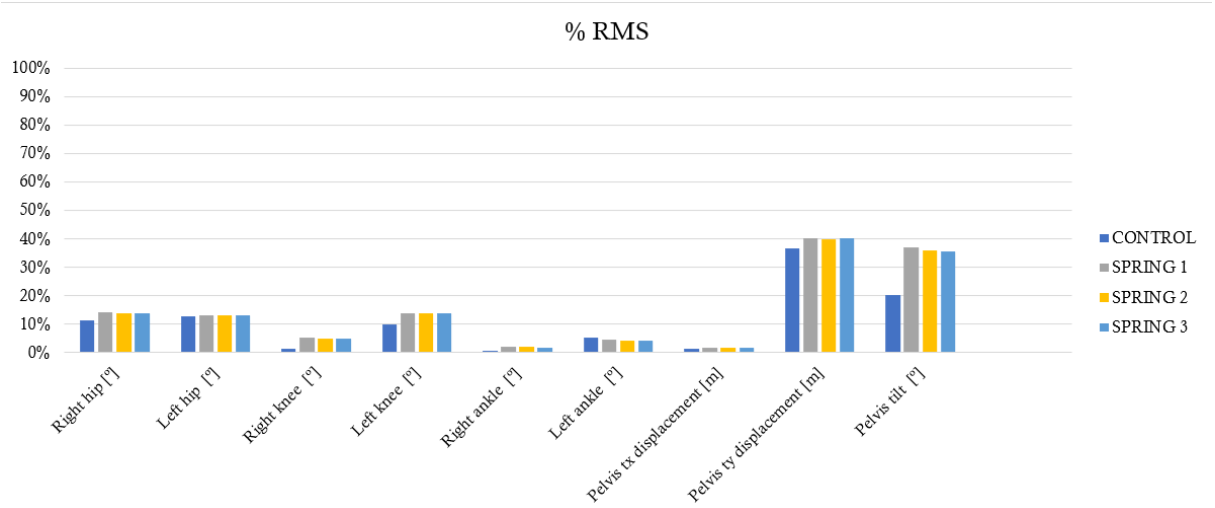

Figure 33: Percentage of the RMS with respect to the reference range of motion in each tracking.

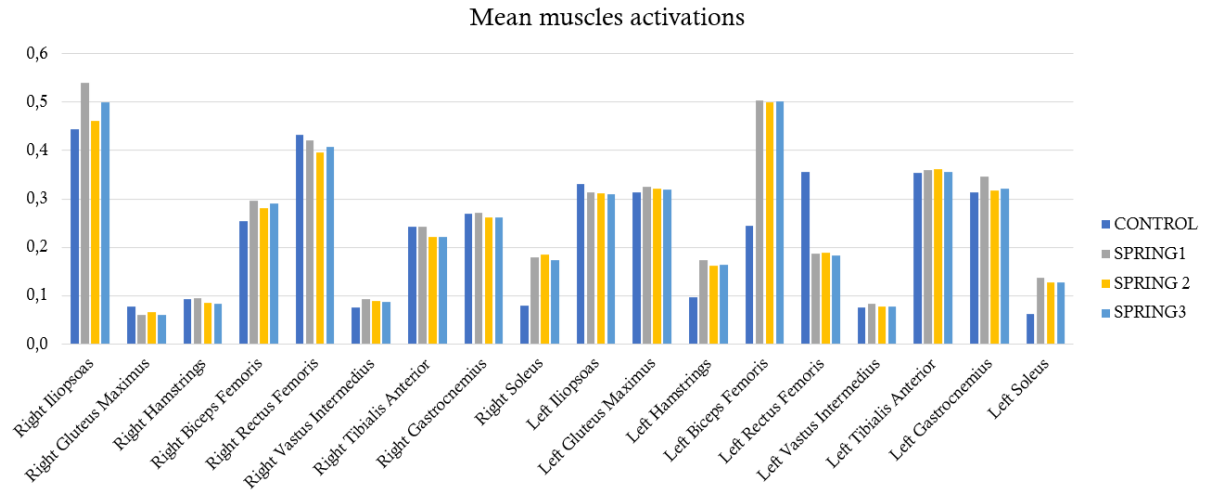

Figure 34: Muscles activations in each tracking.

be a negative outcome.

Lastly, the reserve actuators' torque in the trackings with the springs has considerably reduced in comparison with the *WEAKENED*, although not to the level of the *CONTROL* tracking. This means that the spring helps the model reproducing the movement, but it is still not enough.

The results obtained from the implementation of the device are valued positively because the difference between the reproduced movement and the reference is small enough to accept the simulation as optimal, and the designed *SPRING 2* has helped reduce almost all the muscle activations and specifically the activations of the right iliopsoas, which was the targeted muscle. Therefore, the chosen device is the ***SPRING 2***, with the parameters shown in Table 8.

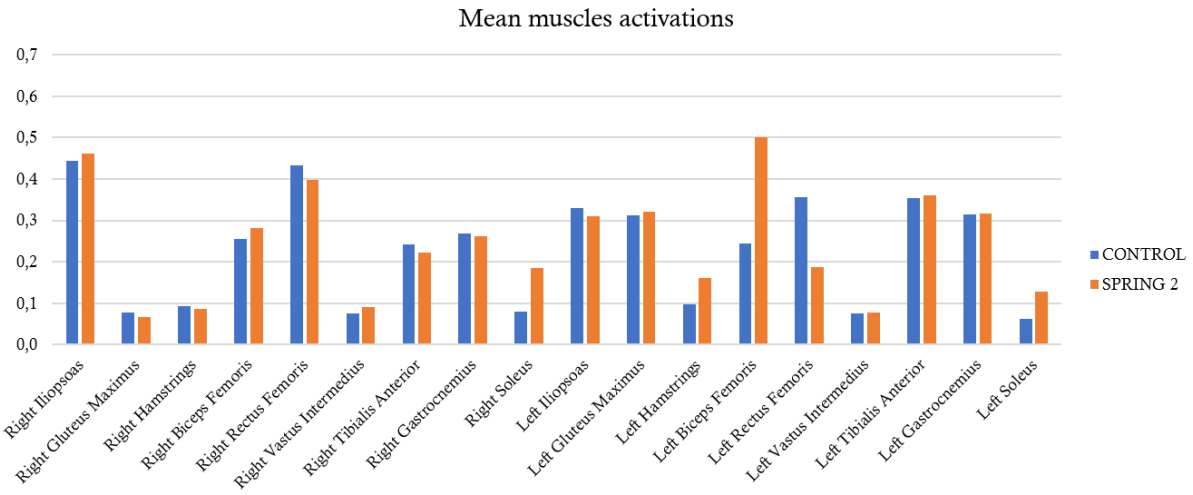

Figure 35: Muscles activations in *CONTROL* and *SPRING 2* tracking.

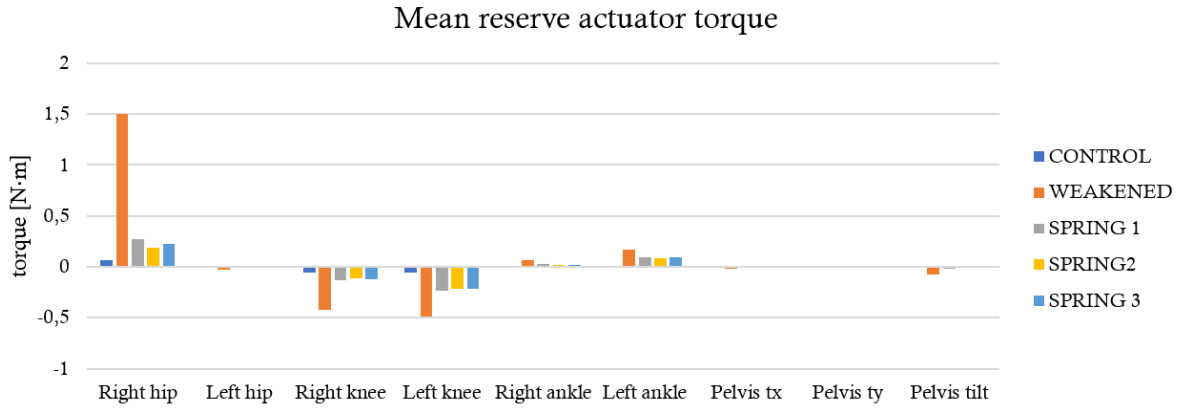

Figure 36: Reserve actuators' performance in each tracking.

	$k\ [N \cdot m/rad]$	$M_0\ [N]$	$\theta_0\ [rad]$
SPRING 2	**5.446**	1.8997	**0.34883**

Table 8: Parameters of the chosen spring.

However, the negative outcomes the spring has in the left biceps femoris is not to be avoided. A possible solution would be the implementation of a similar device in the left hip to help counteract the hyper-activation of the biceps femoris.

4.4 Limitations of the thesis

Some limitations have to be considered when assessing the results of this thesis. Firstly, only one model for the healthy child and one for the child with DMD from a specific age have been used. This limits the extrapolation of the results, as the disease affects very differently depending on the age, and many factors can influence the progression and expression of DMD. In addition to that, it was initially intended to use the data of the oldest children in the study (ten years and six/seven months old), but there was a missing marker in the data, and it caused some problems. Hence, it was then changed to the middle age group (nine years old), thus modifying the initial objective of working with patients who were in the late ambulatory stage.

Secondly, the simplifications of the musculoskeletal model limit the reproduction of the human movement. A 2D model has been used (although the third dimension was added, it was only to be able to use the experimental data), with eighteen muscles that could only reproduce the flexion/extension movements in the joints.

And thirdly, due to the timing of the thesis, only one device was implemented in the model. A simple design was chosen for the device and the parameters for a spring were calculated using first degree lineal regression.

5 Economic cost of the project

Since no data needed to be collected for this project, the economic cost relies on the working time of the student and supervisors, the software's licences, the depreciation of the personal laptop and the electrical energy consumed.

Regarding the working time of the student, 20 hours per week have been dedicated to this project during approximately seven months, which comes to a total of 600 hours in total earning 8€/h, which is the student salary recommended in ETSEIB. As for the supervisor's work, at least one meeting per week has been held, which are approximately 30 hours, and the extra time dedicated to resolving doubts via mail and the thesis correction would add another 10 hours of work, which comes to a total of 40 hours at 50€/h salary.

OpenSim and OpenSim Moco are completely free licenses, whereas the MATLAB license cost is 250€/year for academic use. Regarding the depreciation of the personal laptop, it is estimated 5 years of useful life and a price of 800€. Considering it is used during 52 weeks per year, 8 hours per day and 5 hours per week, it comes to a total of 2080 hours of useful life, which results in a variable cost of 0.3846€/h. Lastly, the electrical energy consumed by the personal laptop is estimated using the working time of the student (600 hours), the power of the laptop of approximately 60W and a constant value of electric energy equal to 0.20€/KWh. The total cost of the project is shown in the following table.

Cost factor	**Work time [h]**	**Cost per hour [€/h]**	**Cost related to the project [€]**
Student	600	8	4800
Supervisor	40	50	2000
MATLAB License			250
Laptop use	600	0.3846	230.76
Electrical energy	600	0.012	5.04
Total cost			**7285.8 €**

Table 9: Economic cost of the project

6 Conclusions

To conclude this thesis, a review of the settled objectives and how they have been achieved will be carried out. The most important results of the thesis will be mentioned, and then the future steps and impact of the thesis will be stated.

A thorough research on the effects of DMD on muscles and gait has been carried out and used to properly model muscle dystrophy in the OpenSim Moco environment. An adult model with ten degrees of freedom has been scaled to the size and properties of a child with DMD and a healthy child. Additionally, six degrees of freedom have been added to the model in order to carry out these adaptations. The experimental data has been processed and used as a reference and as an initial guess for the *MocoTrack* problems. The implementation of the muscular dystrophy in the models has been hypothesized and tested by reducing the maximum isometric force of the models. In order to design, optimize and implement a passive assistive device, the healthy model has been modified by reducing the maximum isometric force to model the muscular dystrophy, and the activations of the muscles have been limited with the purpose of forcing the reserve actuators to perform. The results of the *MocoTrack* carried out with the weakened model have been analysed, and the relation between the highest torque and the muscle weakness has been hypothesized. Then, from the highest reserve actuators' torque, which has been found to be in the right hip, three different devices have been designed using a first order lineal regression, thus making three springs. The three springs have been implemented in the model, and a *MocoTrack* has been carried out with each one of them. The solutions of these trackings have been analysed, and the optimal spring has been defined.

Regarding the results of the thesis, the tracking of the movement with the *DMD* and *CONTROL* models is considered to be correct, especially because of the obtention of higher muscle activations in the *DMD* model, which is valued as a result of a good modelling of the muscular dystrophy. As for the modelling of the muscular dystrophy in the healthy model, it is considered to be a good first approach, which has provided the results needed to design a device and has enabled the development of a hypothesis on the relation between the weakness of the muscles and the performance of the reserve actuators. Concerning the design and optimization of the device, the decreasing of the muscle activation due to the implementation of the chosen device is valued very positively, although the impact on some muscles should be optimized.

With regard to the future steps of this thesis, a more complex musculoskeletal model should be considered. Although the used model has all the muscles necessary to carry out the flexion/extension movements in every joint, adding some more muscles would allow representing better the movement and obtaining more reliable results on the muscle activations. Moreover, more degrees of freedom should be considered for the simulations, given that hip adduction/abduction and pelvis rotation are used by children with DMD to obtain stability while walking. Furthermore, simulations of older children would probably provide more conclusive

results because the kinematic changes exaggerate with the progression of the disease. On the subject of the optimal control techniques, with the tracking solutions obtained in this thesis, predictions of the movements could be implemented. And lastly, relating to the device, there are a few options that could be followed. For instance, more than one device could be implemented in the model, or a more complex device could be designed, thus enabling to substitute better the reserve actuators and probably help more the model. Additionally, the device's parameters could be optimized using Moco. Moreover, the actual implementation of the device should be considered.

Concerning the impact of this thesis, the research carried out on DMD, the code developed, and the results obtained are valuable for following research in the line of this thesis. Musculoskeletal simulations are of great help in the design and development of assistive devices because they allow the visualization and quantification of the impact the devices might have without having to build and test them on patients. In the case of children with DMD, this is especially important because of their physical condition.

For this reason, I hope this project continues forward and a device is built for children with DMD to assist them walking and improve their lives.

References

[1] M. C. Walter and P. Reilich, "Recent developments in Duchenne muscular dystrophy: facts and numbers," *Journal of Cachexia, Sarcopenia and Muscle*, vol. 8, no. 5, pp. 681–685, 2017.

[2] "Human biodigital." [Online]. Available: https://www.biodigital.com/

[3] B. D. CL Vaughan and J. O'Connor, *Dynamics of Human Gait*, 2nd ed. Kiboho, 1992. [Online]. Available: http://www.gaitlab.ir/books/gaitlab_ref_4_Dynamics_of_Human_Gait.pdf

[4] U. Themes, "Right gait cycle," Jun 2016. [Online]. Available: https://musculoskeletalkey.com/gait/

[5] M. Matthews, "This is everything you need to know about anterior pelvic tilt," Apr 2021. [Online]. Available: https://legionathletics.com/anterior-pelvic-tilt/

[6] O. Jones, "Anatomical terms of movement," May 2020. [Online]. Available: https://teachmeanatomy.info/the-basics/anatomical-terminology/terms-of-movement/

[7] S. Preuss, "The direct approach: Treating lower back pain with strength," Feb 2013. [Online]. Available: http://www.thhlblog.com/2013/02/the-direct-approach-treating-lower-back.html

[8] "Medicine and health." [Online]. Available: https://www.chegg.com/flashcards/lower-extremity-pt-1-469577b2-816c-4a49-a6bb-69461135bec9/deck

[9] "Know your knees to help prevent pain and injury." [Online]. Available: https://www.yogajournal.com/teach/anatomy-yoga-practice/know-your-knees-to-help-prevent-pain-and-injury/

[10] "Tratamiento ortopédico para personas con dmd." [Online]. Available: https://www.duchenne-spain.org/tratamiento/tratamiento-ortopedico/

[11] A. Peiret and J. M. Font, "Report on neuromusculoskeletal and contact modelling," 2021.

[12] "Opensim moco." [Online]. Available: https://opensim-org.github.io/opensim-moco-site/

[13] C. L. Dembia, N. A. Bianco, A. Falisse, J. L. Hicks, and S. L. Delp, "OpenSim Moco: Musculoskeletal optimal control," *PLoS Computational Biology*, vol. 16, no. 12 December, pp. 1–25, 2020.

[14] Eurecat, "Entregable E1.2 ANÁLISIS BIOMECÁNICO EN PACIENTES CON DMD," Tech.

Rep., 2017.

[15] "Opensim documentation." [Online]. Available: https://simtk-confluence.stanford.edu/display/OpenSim/OpenSim+Documentation

[16] B. T. Darras, "Patient education: Overview of muscular dystrophies (Beyond the Basics)," *UpToDate*, pp. 1–18, 2018. [Online]. Available: https://www-uptodate-com.uml.idm.oclc.org/contents/overview-of-muscular-dystrophies-beyond-the-basics?search=musculardystrophy&source=search_result&selectedTitle=7$\sim$150&usage_type=default&display_rank=7#H2

[17] P. D. J. Kirschner, "Disease stages," Jan 2010. [Online]. Available: http://www.dmd-guide.org/disease-stages/overview/

[18] "What are the stages of muscular dystrophy?" [Online]. Available: https://www.medicinenet.com/what_are_the_stages_of_muscular_dystrophy/article.htm

[19] "Gower's sign." [Online]. Available: https://neurosigns.org/wiki/Gower%27s_sign

[20] [Online]. Available: https://medical-dictionary.thefreedictionary.com/

[21] M. Goudriaan, M. Van den Hauwe, J. Dekeerle, L. Verhelst, G. Molenaers, N. Goemans, and K. Desloovere, "Gait deviations in duchenne muscular dystrophy—part 1. a systematic review," *Gait and Posture*, vol. 62, pp. 247–261, 2018. [Online]. Available: https://www.sciencedirect.com/science/article/pii/S0966636218301693

[22] M. Goudriaan, M. Van den Hauwe, C. Simon-Martinez, C. Huenaerts, G. Molenaers, N. Goemans, and K. Desloovere, "Gait deviations in duchenne muscular dystrophy—part 2. statistical non-parametric mapping to analyze gait deviations in children with duchenne muscular dystrophy," *Gait and Posture*, vol. 63, pp. 159–164, 2018. [Online]. Available: https://www.sciencedirect.com/science/article/pii/S0966636218304454

[23] EURECAT", Marsi Bionics", Escribano", CSIC", and Hospital Sant Joan de Déu", "EXO-RAPI," 08 2019. [Online]. Available: https://eurecat.org/es/portfolio-items/exorapi/

[24] I. Vandekerckhove, N. De Beukelaer, M. Van den Hauwe, B. R. Shuman, K. M. Steele, A. Van Campenhout, N. Goemans, K. Desloovere, and M. Goudriaan, "Muscle weakness has a limited effect on motor control of gait in duchenne muscular dystrophy," *PLOS ONE*, vol. 15, pp. 1–15, 09 2020. [Online]. Available: https://doi.org/10.1371/journal.pone.0238445

[25] L. Doglio, E. Pavan, I. Pernigotti, P. Petralia, C. Frigo, and C. Minetti, "Early signs of gait deviation in duchenne muscular dystrophy," *European jour-*

nal of physical and rehabilitation medicine, vol. 47, pp. 587–94, 09 2011. [Online]. Available: https://www.researchgate.net/publication/51632480_Early_signs_of_gait_deviation_in_Duchenne_muscular_dystrophy

[26] M. G. D'Angelo, M. Berti, L. Piccinini, M. Romei, M. Guglieri, S. Bonato, A. Degrate, A. C. Turconi, and N. Bresolin, "Gait pattern in duchenne muscular dystrophy," *Gait and Posture*, vol. 29, no. 1, pp. 36–41, 2009. [Online]. Available: https://www.sciencedirect.com/science/article/pii/S0966636208001525

[27] Dra. Julita Medina, "Avanç De La Distròfia Muscular De Duchenne," Personal communication, March 2021, Servei de Medicina Física i Rehabilitació, Hospital Universitari Sant Joan de Deu.

[28] O. Alís, "Treball de Final de Grau amb Duchenne," Personal communication, March 2021.

[29] N. Gaudreault, D. Gravel, S. Nadeau, S. Houde, and D. Gagnon, "Gait patterns comparison of children with duchenne muscular dystrophy to those of control subjects considering the effect of gait velocity," *Gait and Posture*, vol. 32, no. 3, pp. 342–347, 2010. [Online]. Available: https://www.sciencedirect.com/science/article/pii/S096663621000161X

[30] Eurecat, "Entregable E1.1 BIOMECÁNICA DE LA MARCHA EN DUCHENNE," Tech. Rep., 2016.

[31] J. Ropars, M. Lempereur, C. Vuillerot, V. Tiffreau, S. Peudenier, J.-M. Cuisset, Y. Pereon, F. Leboeuf, L. Delporte, Y. Delpierre, R. Gross, and S. Brochard, "Muscle activation during gait in children with duchenne muscular dystrophy," *PLOS ONE*, vol. 11, no. 9, pp. 1–13, 09 2016. [Online]. Available: https://doi.org/10.1371/journal.pone.0161938

[32] E. Bosch, "Anàlisi dinàmica inversa del moviment humà mitjançant el programari Opensim," 2013.

[33] N. Rina, "Development of an optimal control framework to predict human motion," Jun 2020.

[34] "Thelen 2003 muscle model." [Online]. Available: https://simtk-confluence.stanford.edu/display/OpenSim/Thelen+2003+Muscle+Model

[35] B. Malizia, P. Ryali, and J. Patton, "Passive Exotendon Spring Elements can replace Muscle Torque during Gait," *Proceedings of the IEEE RAS and EMBS International Conference on Biomedical Robotics and Biomechatronics*, vol. 2020-Novem, pp. 773–778, 2020.

[36] S. H. Collins, M. Bruce Wiggin, and G. S. Sawicki, "Reducing the energy cost of human walking using an unpowered exoskeleton," *Nature*, vol. 522, no. 7555, pp. 212–215, 2015.

A Plots and results

In this annex. the values used for the plots in 4 are exposed in tables. For each tracking there is: a table with the RMS, range of motion of the reference and the $\%RMS$; a table with the mean, maximum and minimum values of the torques applied by the reserve actuators; and a table with the mean, maximum and minimum values of the right and left muscles' activations.

A.1 Tracking of the movement

A.1.1 *DMD* model

Coordinate	RMS	Range of motion of the reference	% RMS
Right hip [º]	1.64371	41.14699	3.99473%
Left hip [º]	1.68390	47.08089	3.57661%
Right knee [º]	2.05024	63.78937	3.21409%
Left knee [º]	1.74097	59.45256	2.92834%
Right ankle [º]	0.40030	27.95773	1.43180%
Left ankle [º]	0.65449	30.38021	2.15434%
Pelvis tx displacement [m]	0.02911	0.59268	4.91111%
Pelvis ty displacement [m]	0.00320	0.02087	15.33372%
Pelvis tilt [º]	1.31747	4.25922	30.93215%

Table 10: Root Mean Square of the coordinates of the *DMD* tracking, the range of motion of the reference in each coordinate, and the percentage of the RMS respect the range of motion.

Reserve actuators	Mean [N·m]	Maximum [N·m]	Minimum [N·m]
Right hip	0.01186	0.54276	-0.27072
Left hip	0.04122	0.28248	-0.54785
Right knee	-0.01930	1.08720	-0.82052
Left knee	0.01420	1.85678	-0.92093
Right ankle	-0.00532	0.25272	-0.20501
Left ankle	-0.06319	0.32137	-0.51557
Pelvis tx	-0,00245	0,009093	-0,01555
Pelvis ty	0,022203	0,036102	-0,00343
Pelvis tilt	-0,01765	0,038099	-0,08827

Table 11: Torque values of the reserve actuators in the *DMD* tracking.

	Activation values		
Muscles	**Mean**	**Maximum**	**Minimum**
Right Iliopsoas	0.42964	0.85902	0.13155
Right Gluteus Maximus	0.45375	0.75841	0.14429
Right Hamstrings	0.37265	0.53816	0.22414
Right Biceps Femoris	0.47454	0.76375	0.12269
Right Rectus Femoris	0.52199	0.95525	0.17533
Right Vastus Intermedius	0.38389	0.83880	0.05156
Right Tibialis Anterior	0.44160	0.75770	0.14662
Right Gastrocnemius	0.39429	0.66900	0.12071
Right Soleus	0.43393	0.87810	0.12840
Left Iliopsoas	0.51775	0.68824	0.15555
Left Gluteus Maximus	0.32099	0.84456	0.07741
Left Hamstrings	0.33680	0.44459	0.17181
Left Biceps Femoris	0.47873	0.78345	0.07733
Left Rectus Femoris	0.57531	0.96068	0.06828
Left Vastus Intermedius	0.35927	0.93251	0.02828
Left Tibialis Anterior	0.35492	0.63617	0.07617
Left Gastrocnemius	0.39869	0.75452	0.13329
Left Soleus	0.53749	0.93143	0.13773

Table 12: Right and left muscle activations in the *DMD* tracking.

A.1.2 *CONTROL* model

Coordinate	RMS	Range of motion of the reference	% RMS
Right hip [º]	6.44187	56.27513	11.44710%
Left hip [º]	7.41021	59.05711	12.54754%
Right knee [º]	1.04064	78.56210	1.32461%
Left knee [º]	7.89157	79.18401	9.96612%
Right ankle [º]	0.16071	24.59134	0.65352%
Left ankle [º]	1.09128	20.23975	5.39178%
Pelvis tx displacement [m]	0.01175	0.89986	1.30616%
Pelvis ty displacement [m]	0.01122	0.03057	36.69070%
Pelvis tilt [º]	0.94828	4.68598	20.23657%

Table 13: Root Mean Square of the coordinates of the *CONTROL* tracking, the range of motion of the reference in each coordinate, and the percentage of the RMS with respect to the range of motion.

Reserve actuators	Mean [N·m]	Maximum [N·m]	Minimum [N·m]
Right hip	0.061958	0.554305	-0.05205
Left hip	0.003701	0.324346	-0.22623
Right knee	-0.0554	0.247072	-0.45496
Left knee	-0.05158	0.172618	-0.24045
Right ankle	0.004132	0.300783	-0.18444
Left ankle	0.012829	0.129096	-0.14109
Pelvis tx	-0,00967	0,037872	-0,07179
Pelvis ty	-0,01294	0,009631	-0,04588
Pelvis tilt	0,006633	0,143524	-0,1018

Table 14: Torque values of the reserve actuators in the *CONTROL* tracking.

	Activation values		
Muscles	**Mean**	**Maximum**	**Minimum**
Right Iliopsoas	0.44396	0.99661	0.11533
Right Gluteus Maximus	0.07654	0.80507	0.01045
Right Hamstrings	0.09180	0.37462	0.02454
Right Biceps Femoris	0.25480	0.78778	0.03568
Right Rectus Femoris	0.43183	0.99533	0.01430
Right Vastus Intermedius	0.07491	0.27995	0.01071
Right Tibialis Anterior	0.24289	0.99069	0.02078
Right Gastrocnemius	0.26918	0.98262	0.01223
Right Soleus	0.07928	0.21567	0.01587
Left Iliopsoas	0.33083	0.99674	0.01136
Left Gluteus Maximus	0.31298	0.75132	0.01531
Left Hamstrings	0.09619	0.26144	0.01201
Left Biceps Femoris	0.24348	0.55179	0.02799
Left Rectus Femoris	0.35546	0.99346	0.01509
Left Vastus Intermedius	0.07471	0.24502	0.02771
Left Tibialis Anterior	0.35318	0.98514	0.04479
Left Gastrocnemius	0.31426	0.92795	0.01525
Left Soleus	0.06188	0.21717	0.01124

Table 15: Right and left muscle activations in the *CONTROL* tracking.

A.2 DMD modelling

Coordinate	RMS	Range of motion of the reference	% RMS
Right hip [º]	10.35489	56.27513	18.400%
Left hip [º]	10.46714	59.05711	17.724%
Right knee [º]	5.71381	78.56210	7.273%
Left knee [º]	13.00977	79.18401	16.430%
Right ankle [º]	0.35601	24.59134	1.448%
Left ankle [º]	1.09128	20.23975	5.392%
Pelvis tx displacement [m]	0.01539	0.89986	1.710%
Pelvis ty displacement [m]	0.01126	0.03057	36.839%
Pelvis tilt [º]	3.30594	4.68598	70.550%

Table 16: Root Mean Square of the coordinates of the *WEAKENED* tracking, the range of motion of the reference in each coordinate, and the percentage of the RMS with respect to the range of motion.

The reserve actuator's performance in the *WEAKENED* model has already been exposed in the text in Table 4.

	Activation values		
Muscles	**Mean**	**Maximum**	**Minimum**
Right Iliopsoas	0.44986	0.49943	0.20606
Right Gluteus Maximus	0.05026	0.30644	0.01069
Right Hamstrings	0.12110	0.39329	0.01746
Right Biceps Femoris	0.30007	0.49126	0.02131
Right Rectus Femoris	0.34923	0.49903	0.08961
Right Vastus Intermedius	0.11981	0.47272	0.01062
Right Tibialis Anterior	0.19854	0.49199	0.01676
Right Gastrocnemius	0.19516	0.49671	0.01357
Right Soleus	0.18941	0.47540	0.01151
Left Iliopsoas	0.21027	0.49733	0.01123
Left Gluteus Maximus	0.21881	0.49635	0.01562
Left Hamstrings	0.22603	0.49786	0.03633
Left Biceps Femoris	0.31554	0.49365	0.01988
Left Rectus Femoris	0.16099	0.49465	0.01281
Left Vastus Intermedius	0.12363	0.47122	0.01369
Left Tibialis Anterior	0.25575	0.49743	0.02406
Left Gastrocnemius	0.21089	0.49386	0.01657
Left Soleus	0.16937	0.47869	0.01117

Table 17: Right and left muscle activations in the *WEAKENED* tracking.

A.3 Design of the device

A.3.1 SPRING 1

Coordinate	RMS	Range of motion of the reference	% RMS
Right hip [º]	7.98268	56.27513	14.185%
Left hip [º]	7.66467	59.05711	12.978%
Right knee [º]	4.02881	78.56210	5.128%
Left knee [º]	10.93042	79.18401	13.804%
Right ankle [º]	0.51700	24.59134	2.102%
Left ankle [º]	0.90924	20.23975	4.492%
Pelvis tx displacement [m]	0.01477	0.89986	1.642%
Pelvis ty displacement [m]	0.01233	0.03057	40.322%
Pelvis tilt [º]	1.72549	4.68598	36.822%

Table 18: Root Mean Square of the coordinates of the *SPRING 1* tracking, the range of motion of the reference in each coordinate, and the percentage of the RMS with respect to the range of motion.

Reserve actuators	Mean [N·m]	Maximum [N·m]	Minimum [N·m]
Right hip	0.270679	1.647254	-0.13032
Left hip	0.008355	0.609652	-0.60584
Right knee	-0.13357	0.362794	-1.22488
Left knee	-0.23317	0.452676	-0.84742
Right ankle	0.028241	0.297914	-0.20534
Left ankle	0.093418	0.543653	-0.14038
Pelvis tx	-0,00335	0,008836	-0,03896
Pelvis ty	0,001628	0,014447	-0,03358
Pelvis tilt	-0,01854	0,095951	-0,1201

Table 19: Torque values of the reserve actuators in the *SPRING 1* tracking.

	Activation values		
Muscles	**Mean**	**Maximum**	**Minimum**
Right Iliopsoas	0.54045	0.99873	0.04464
Right Gluteus Maximus	0.06079	0.53575	0.01077
Right Hamstrings	0.09410	0.31889	0.02147
Right Biceps Femoris	0.29696	0.96941	0.05687
Right Rectus Femoris	0.42195	0.99645	0.02355
Right Vastus Intermedius	0.09270	0.36028	0.01144
Right Tibialis Anterior	0.24228	0.99319	0.01968
Right Gastrocnemius	0.27054	0.99386	0.01673
Right Soleus	0.17914	0.59623	0.01335
Left Iliopsoas	0.31434	0.99610	0.01115
Left Gluteus Maximus	0.32531	0.98924	0.01667
Left Hamstrings	0.17251	0.57065	0.01928
Left Biceps Femoris	0.50397	0.97519	0.02859
Left Rectus Femoris	0.18633	0.64407	0.01341
Left Vastus Intermedius	0.08406	0.30541	0.01664
Left Tibialis Anterior	0.36035	0.98777	0.02380
Left Gastrocnemius	0.34584	0.96484	0.02502
Left Soleus	0.13621	0.74571	0.01193

Table 20: Right and left muscle activations in the *SPRING 1* tracking.

A.3.2 SPRING 2

Coordinate	RMS	Range of motion of the reference	% RMS
Right hip [º]	7.72439	56.27513	13.726%
Left hip [º]	7.67081	59.05711	12.989%
Right knee [º]	3.89135	78.56210	4.953%
Left knee [º]	10.79406	79.18401	13.632%
Right ankle [º]	0.50909	24.59134	2.070%
Left ankle [º]	0.84151	20.23975	4.158%
Pelvis tx displacement [m]	0.01529	0.89986	1.699%
Pelvis ty displacement [m]	0.01219	0.03057	39.860%
Pelvis tilt [º]	1.68109	4.68598	35.875%

Table 21: Root Mean Square of the coordinates of the *SPRING 2* tracking, the range of motion of the reference in each coordinate, and the percentage of the RMS with respect to the range of motion.

Reserve actuators	Mean [N·m]	Maximum [N·m]	Minimum [N·m]
Right hip	0.190705	1.386679	-0.07602
Left hip	0.009241	0.664004	-0.54458
Right knee	-0.11232	0.323242	-1.06498
Left knee	-0.21582	0.26736	-0.87585
Right ankle	0.020865	0.308371	-0.44703
Left ankle	0.086281	0.344232	-0.17878
Pelvis tx	-0,00193	0,004857	-0,01098
Pelvis ty	0,000659	0,008546	-0,00319
Pelvis tilt	-0,00761	0,043705	-0,08336

Table 22: Torque values of the reserve actuators in the *SPRING 2* tracking.

	Activation values		
Muscles	**Mean**	**Maximum**	**Minimum**
Right Iliopsoas	0.46113	0.99879	0.04278
Right Gluteus Maximus	0.06641	0.77722	0.01048
Right Hamstrings	0.08567	0.38309	0.01777
Right Biceps Femoris	0.28101	0.96573	0.03927
Right Rectus Femoris	0.39683	0.99597	0.01779
Right Vastus Intermedius	0.08976	0.39003	0.01076
Right Tibialis Anterior	0.22216	0.99724	0.01463
Right Gastrocnemius	0.26258	0.99547	0.01321
Right Soleus	0.18421	0.66052	0.01212
Left Iliopsoas	0.31101	0.99728	0.01068
Left Gluteus Maximus	0.32112	0.99307	0.01417
Left Hamstrings	0.16107	0.52256	0.01490
Left Biceps Femoris	0.50044	0.98073	0.02055
Left Rectus Femoris	0.18783	0.63410	0.01168
Left Vastus Intermedius	0.07658	0.29893	0.01772
Left Tibialis Anterior	0.36107	0.99533	0.01757
Left Gastrocnemius	0.31647	0.96400	0.01817
Left Soleus	0.12721	0.71711	0.01029

Table 23: Right and left muscle activations in the *SPRING 2* tracking.

A.3.3 SPRING 3

Coordinate	RMS	Range of motion of the reference	% RMS
Right hip [º]	7.80555	56.27513	13.870%
Left hip [º]	7.66482	59.05711	12.979%
Right knee [º]	3.93974	78.56210	5.015%
Left knee [º]	10.80274	79.18401	13.643%
Right ankle [º]	0.40339	24.59134	1.640%
Left ankle [º]	0.86983	20.23975	4.298%
Pelvis tx displacement [m]	0.01502	0.89986	1.669%
Pelvis ty displacement [m]	0.01228	0.03057	40.172%
Pelvis tilt [º]	1.66817	4.68598	35.599%

Table 24: Root Mean Square of the coordinates of the *SPRING 3* tracking, the range of motion of the reference in each coordinate, and the percentage of the RMS with respect to the range of motion.

Reserve actuators	Mean [N·m]	Maximum [N·m]	Minimum [N·m]
Right hip	0.22322	1.48423	-0.14063
Left hip	0.00721	0.64954	-0.67430
Right knee	-0.11988	0.31931	-1.10343
Left knee	-0.21597	0.32120	-0.84781
Right ankle	0.02114	0.30818	-0.48861
Left ankle	0.09017	0.34295	-0.18477
Pelvis tx	-0,00137	0,003828	-0,00476
Pelvis ty	-0,00057	0,003203	-0,00433
Pelvis tilt	-0,00899	0,038452	-0,09029

Table 25: Torque values of the reserve actuators in the *SPRING 3* tracking.

	Activation values		
Muscles	**Mean**	**Maximum**	**Minimum**
Right Iliopsoas	0.50043	0.99902	0.04823
Right Gluteus Maximus	0.06100	0.71302	0.01048
Right Hamstrings	0.08235	0.36404	0.01771
Right Biceps Femoris	0.29013	0.96982	0.04015
Right Rectus Femoris	0.40841	0.99650	0.01826
Right Vastus Intermedius	0.08644	0.35539	0.01082
Right Tibialis Anterior	0.22151	0.99752	0.01546
Right Gastrocnemius	0.26137	0.99525	0.01290
Right Soleus	0.17319	0.61896	0.01219
Left Iliopsoas	0.30991	0.99720	0.01067
Left Gluteus Maximus	0.31854	0.99284	0.01435
Left Hamstrings	0.16309	0.55198	0.01524
Left Biceps Femoris	0.50227	0.98113	0.02150
Left Rectus Femoris	0.18364	0.60495	0.01190
Left Vastus Intermedius	0.07655	0.29956	0.01834
Left Tibialis Anterior	0.35596	0.99469	0.01850
Left Gastrocnemius	0.32114	0.96578	0.01887
Left Soleus	0.12748	0.73416	0.01030

Table 26: Right and left muscle activations in the *SPRING 3* tracking.